bioRxiv preprint doi: https://doi.org/10.1101/603555; this version posted April 9, 2019. The copyright holder for this preprint (which was not certified by peer review) is the author/funder, who has granted bioRxiv a license to display the preprint in perpetuity. It is made available under aCC-BY-NC-ND 4.0 International license.

Subcellular compartments interplay for carbon and nitrogen allocation in *Chromera velia* and *Vitrella brassicaformis*

Zoltán Füssy[1,2,*], Tereza Faitová[2,3], and Miroslav Oborník[1,2,*]

[1]Faculty of Science, University of South Bohemia, České Budějovice, Czech Republic

[2]Institute of Parasitology, Biology Centre CAS, České Budějovice, Czech Republic

[3]Faculty of Engineering and Natural Sciences, Johannes Kepler University, Linz, Austria

* corresponding authors: zoltan.fussy@gmail.com, obornik@paru.cas.cz

ABSTRACT

Endosymbioses necessitate functional cooperation of cellular compartments to avoid pathway redundancy and streamline the control of biological processes. To gain insight into the metabolic compartmentation in chromerids, phototrophic relatives to apicomplexan parasites, we prepared a reference set of proteins probably localized to mitochondria, cytosol and the plastid, taking advantage of available genomic and transcriptomic data. Training of prediction algorithms with the reference set now allows a genome-wide analysis of protein localization in *C. velia* and *V. brassicaformis*. We found that the chromerid plastids house enzymatic pathways needed for their maintenance and photosynthetic activity, but for carbon and nitrogen allocation, metabolite exchange is necessary with the cytosol and mitochondria. This indeed suggests that the regulatory mechanisms operate in the cytosol to control carbon metabolism based on the availability of both light and nutrients. We discuss that this arrangement is largely

bioRxiv preprint doi: https://doi.org/10.1101/603555; this version posted April 9, 2019. The copyright holder for this preprint (which was not certified by peer review) is the author/funder, who has granted bioRxiv a license to display the preprint in perpetuity. It is made available under aCC-BY-NC-ND 4.0 International license.

shared with apicomplexans, possibly stemming from a common ancestral metabolic architecture, and supports the mixotrophy of the chromerid algae.

KEYWORDS: chromerid, protein localization, prediction algorithm, endosymbiosis, plastid integration, mixotrophy

bioRxiv preprint doi: https://doi.org/10.1101/603555; this version posted April 9, 2019. The copyright holder for this preprint (which was not certified by peer review) is the author/funder, who has granted bioRxiv a license to display the preprint in perpetuity. It is made available under aCC-BY-NC-ND 4.0 International license.

INTRODUCTION

Endosymbiotic organelles play crucial roles in cellular biochemistry. Mitochondria, alpha-proteobacterial endosymbionts of eukaryotes (Oborník 2019; Gruber 2019), represent an energetic hub, where balancing of catabolic and anabolic processes takes place tightly regulated with the speed of respiration (e.g. Searcy 2003; Pagliarini and Rutter 2013; Gray 2015). In plastids, domesticated cyanobacteria (Gruber 2019; Oborník 2019), inorganic carbon is fixed into sugars and several essential compounds are synthesized, such as fatty acids, isoprenoid units, tetrapyrroles, and amino acids (e.g. Tetlow et al. 2017). These semiautonomous endosymbiont-derived organelles contain genetic information and their own translation apparatuses, but by far do not encode all the proteins required for their function. Due to endosymbiotic gene transfer, most essential genes were transferred from their genomes to the nuclear genome and the organelles are greatly dependent on the import of proteins synthesized in the cytosol (e.g. Mallo et al. 2018). Sorting of proteins to subcellular locations specifically is therefore crucial for the correct function of both the proteins and the organelles, and thus targeting signals and protein translocation are key to our understanding of organellar biology (Kunze & Berger 2015).

Reconstruction of ancestral traits (Joy et al. 2016) allows us to unveil changes in lifestyle and genome organization in an evolutionary perspective and to compare functionalities among the organisms of interest. The discovery and genome characterization of chromerids *Chromera velia* and *Vitrella brassicaformis*, the closest known photosynthetic relatives of apicomplexan parasites, have provided an excellent framework to study the transition from free-living phototrophs to obligate parasites (Moore et al. 2008; Oborník et al. 2009; Janouškovec et al. 2010; Burki et al. 2012; Janouškovec et al. 2015; Woo et al. 2015; Füssy & Oborník 2017b). Much knowledge has

bioRxiv preprint doi: https://doi.org/10.1101/603555; this version posted April 9, 2019. The copyright holder for this preprint (which was not certified by peer review) is the author/funder, who has granted bioRxiv a license to display the preprint in perpetuity. It is made available under aCC-BY-NC-ND 4.0 International license.

accumulated about the function of the apicomplexan remnant plastid, the apicoplast (reviewed in Boucher et al. 2018), which given their shared origin structurally and molecularly resembles the photosynthetic plastid of chromerids (Moore et al. 2008; Janouškovec et al. 2010; Woo et al. 2015). Nevertheless, the protein composition of the chromerid plastid is largely unknown, except for a recent work that focused on *C. velia* photosystems (Sobotka et al. 2017), and therefore a pre-transition model of the apicoplast could not be studied in detail. The mitochondrial genome of apicomplexans is massively reduced in gene content and found to contain only three protein-coding genes, *cox1*, *cox3* and *cyb*, with the majority of mitochondrial proteins requiring import from cytosol (Nash et al. 2008; Janouškovec et al. 2013; Flegontov et al. 2015). Strikingly, the *C. velia* mitochondrion was found to contain only two of these genes, *cox1* and *cox3* (Flegontov et al. 2015). It has been hypothesized that the reduction of the apicomplexan (and chromerid) mitochondrial genome could be linked with the change in lifestyle strategy, particularly a change to facultative anaerobiosis (Dorrell et al. 2013), which is consistent with the observed reduction of the respiratory chain in all myzozoans (dinoflagellates, chromerids and apicomplexans) (Flegontov et al. 2015; Oborník & Lukeš 2015).

The relatively small nuclear genome size (up to 193 Mb) and largely complete sequence data of chromerids (Woo et al. 2015) make them ideal for large-scale targeting signal recognition and, by extension, organellar proteome prediction. Up to now, plastid proteomes have been determined in only a handful of organisms, mainly plants and green algae (van Wijk & Baginsky 2011; Terashima et al. 2011; Dorrell et al. 2017), but also a handful of complex algae and protist parasites (Hopkins et al. 2012; Boucher et al. 2018). Similarly, mitochondrial proteomic data are rather scarce and focused on model organisms, such as humans (Calvo & Mootha 2010; Palmfeldt & Bross 2017), yeast

bioRxiv preprint doi: https://doi.org/10.1101/603555; this version posted April 9, 2019. The copyright holder for this preprint (which was not certified by peer review) is the author/funder, who has granted bioRxiv a license to display the preprint in perpetuity. It is made available under aCC-BY-NC-ND 4.0 International license.

(Gonczarowska-Jorge et al. 2017), plants (Huang et al. 2013), and protists (Smith et al. 2007; Atteia et al. 2009; Panigrahi et al. 2009; Danne et al. 2013; Gawryluk et al. 2014).

The aim of the work is to define and characterize the subcellular proteomes of chromerids by bioinformatic tools with an emphasis on plastid- and mitochondrion-destined proteins. For the analysis, we compiled sets of compartment-specific proteins of *C. velia* and *V. brassicaformis* and optimized the performance of the ASAFind (Gruber et al. 2015) prediction tool with the reference amino acid frequency matrices. Our analyses bring first implications on carbon and nitrogen allocation among the plastid, cytosol and mitochondria in chromerids, suggesting interplay of these compartments is in place for efficient carbon metabolism under changing light and nutrient conditions. This work also identifies biochemical peculiarities ancestrally shared with apicomplexans, such as the lack of the canonical mitochondrial pyruvate decarboxylase and cytosolic amino acid synthesis.

DATA SOURCES AND METHODS

The sequence data of the chromerid algae *Chromera velia* CCMP2878 and *Vitrella brassicaformis* CCMP3155 were retrieved from CryptoDB (www.cryptodb.org, version 34). Additional transcriptomic data were retrieved from NCBI GenBank (Dorrell et al. 2014; Woehle et al. 2011) and MMETSP sequence databases (MMETSP0290 and MMETSP1451, (Keeling et al. 2014; Cohen et al. 2016). The sequence data were annotated using the information available at KEGG servers (Kanehisa et al. 2017) and using InterProScan annotation tool of Geneious (Jones et al. 2014; Kearse et al. 2012).

To define the best tool for the subcellular localization of proteins, the sets of reference sequences of *Chromera* and *Vitrella* were analyzed by prediction algorithms. The tools tested were selected to be suitable for large-scale analyses and included:

bioRxiv preprint doi: https://doi.org/10.1101/603555; this version posted April 9, 2019. The copyright holder for this preprint (which was not certified by peer review) is the author/funder, who has granted bioRxiv a license to display the preprint in perpetuity. It is made available under aCC-BY-NC-ND 4.0 International license.

TargetP (Emanuelsson et al. 2000), SignalP (v. 4.1) (Petersen et al. 2011), ASAFind (Gruber et al. 2015), HECTAR v1.3 (Gschloessl et al. 2008), MultiLoc2 (Blum et al. 2009), PrediSi (Hiller et al. 2004) and PredSL (Petsalaki et al. 2006). All the prediction algorithms except HECTAR were run locally with default parameters; SignalP was run with sensitive cutoff values (-u 0.3 -U 0.3). The sensitivity (proportion of recognized true positives) and precision (proportion of positive results, also termed the positive predictive value) of the prediction algorithms were compared, setting a certain threshold specified for each of the predictors. Sensitivity was computed as:

(Eq.1) *sensitivity = (true positives) / (true positives + false negatives)*

and positive predictive value was computed as:

(Eq.2) *precision = (true positives) / (true positives + false positives).*

An optimal threshold would cover maximum positive proteins while including a low number of false positives (proteins falsely predicted to the organelle in question).

Bit score-weighted matrices of amino acid positions surrounding the signal cleavage sites were calculated separately for *C. velia* and *V. brassicaformis*, as described by Crooks et al. (2004). Only cleavage sites which were consensually (by majority agreement) predicted by PrediSi, PredSL, SignalP and ASAFind were considered. The transit peptide sequence logos and frequency plots of plastid-targeted proteins from *C. velia* and *V. brassicaformis* were created with WebLogo (Crooks et al. 2004; http://weblogo.berkeley.edu/; version 2.8.2).

Where applicable, closest hits for proteins were found using BLAST against nr or RefSeq databases, and using DIAMOND (Buchfink et al. 2014) against an in-house made database consisting from sequences collected from NCBI, MMETSP (Keeling et al. 2014; Cohen et al. 2016) and Ensembl Genomes (release 37; Kersey et al. 2016). Sequences were aligned using MAFFT v.7 (Katoh & Standley 2013) and automatically trimmed by

bioRxiv preprint doi: https://doi.org/10.1101/603555; this version posted April 9, 2019. The copyright holder for this preprint (which was not certified by peer review) is the author/funder, who has granted bioRxiv a license to display the preprint in perpetuity. It is made available under aCC-BY-NC-ND 4.0 International license.

trimAL (Capella-Gutiérrez et al. 2009). Maximum likelihood trees were inferred from the trimmed alignments using the best-fitting substitution model as determined by the IQ-TREE –m TEST option limited to LG matrix by -mset (Nguyen et al. 2015). Branch supports were determined by rapid bootstrapping followed by 1,000 ultra-fast bootstrap replicates (-bb 1000).

RESULTS

Sequence completeness and reference compilation

Proteins destined to plastids and mitochondria typically encode an N-terminal motif, i.e. a targeting presequence. The targeting presequence of mitochondrial proteins is termed the mitochondrial transit peptide (mTP) and has the physicochemical properties of an amphiphilic helix. Similarly, the chloroplast transit peptides of primary algae (rhodophytes, chlorophytes and glaucophytes) and plants are amphiphilic helices, though they are typically enriched in hydroxylated amino acids and less positively charged than mTPs (Kunze & Berger 2015; Garg & Gould 2016). In comparison, complex algae (those that maintain eukaryote-eukaryote endosymbionts) including the chromerids, target proteins to the plastid via the endomembrane (secretory) pathway, using chloroplast transit peptides directly preceded by an ER signal peptide, which are referred to as bipartite targeting sequences (BTS) (reviewed in Patron & Waller 2007). To predict a protein's localization to plastid or mitochondria, it is therefore essential to identify its complete N-terminus.

During the annotation and alignment of reference proteins, we noticed that some contigs retrieved from CryptoDB (Woo et al. 2015) are apparently truncated at their 5'-ends. The sequence data appear gene-rich but are still highly fragmented, with 5,966

bioRxiv preprint doi: https://doi.org/10.1101/603555; this version posted April 9, 2019. The copyright holder for this preprint (which was not certified by peer review) is the author/funder, who has granted bioRxiv a license to display the preprint in perpetuity. It is made available under aCC-BY-NC-ND 4.0 International license.

and 1,064 genomic scaffolds assembled for *C. velia* and *V. brassicaformis*, respectively, although the number of chromosomes in *C. velia* is estimated to be much smaller (Vazač et al. 2017). To have an independent assessment of N-termini completeness, we searched for (almost) identical transcripts in chromerid transcriptomes available in GenBank and MMETSP and used these contigs to extend those from CryptoDB towards their 5'-end, where possible. While these fused contigs are indeed chimeras of orthologs from different strains (the transcripts were not completely identical), we assume they code for *bona fide* N-termini in all these sequenced strains of *C. velia* and *V. brassicaformis*. These chimeric contigs are for clear distinction marked in the reference sequence list (Supplementary Table S1; see Supplementary Data S1 where these sequences are listed). Other, apparently truncated contigs were omitted from the reference sets.

We performed a systematic search of housekeeping and metabolically active proteins to obtain the reference sets from *C. velia* and *V. brassicaformis* data. To find plastid references, we searched for pathways intimately linked with their biogenesis and photosynthesis, including the biosynthesis of fatty acids (type II FAS) and lipids, iron-sulfur clusters, terpenoids and terpenoid derivatives (photosynthetic pigments, vitamins), tetrapyrrole cofactors, protein translocator subunits and components of the photosynthetic electron transport chain (recently characterized by Sobotka et al. 2017) (Fig. 1), and the enzymes of carbon fixation (Fig. 2). Among mitochondrial pathways, we looked for the enzymes of the tricarboxylic acid (TCA) cycle and the components of the respiratory chain (Flegontov et al. 2015) (Fig. 2). From pathways localized in the cytosol, we identified the enzymes of glycolysis, storage amylopectin biosynthesis and breakdown (Coppin et al. 2005), and the enzymes of the pentose phosphate cycle that we distinguished from the enzymes of the plastid carbon fixation (Fig. 2). Using

bioRxiv preprint doi: https://doi.org/10.1101/603555; this version posted April 9, 2019. The copyright holder for this preprint (which was not certified by peer review) is the author/funder, who has granted bioRxiv a license to display the preprint in perpetuity. It is made available under aCC-BY-NC-ND 4.0 International license.

phylogenetic analyses (not shown), we also identified ribosomal proteins from all three translationally active compartments (Gupta et al. 2014). We also included biosynthesis pathways of several amino acids and other compounds, where enzymatic steps showed consistent localization (Fig. 2). Organellar genome-encoded proteins were dropped from the reference sets (Supplementary Table 1). In a scarcity of experimental data, we believe this is the most reliable approach to compile reference sequences.

[insert Fig. 1]

Though most of the searched pathways are near-complete, we failed to identify representatives of some enzymatic steps. These include the acyl-[acyl carrier protein (ACP)] ligase (in both chromerids) and two lipid phosphatases of the glycero(phospho)lipid biosynthesis (phosphatidate phosphatase in *C. velia*, phosphatidylglycerophosphatase in *V. brassicaformis*), several enzymes of the carotenoid (neoxanthin synthase), terpenoid-quinone (tocopherol cyclase), and amino acid biosynthesis pathways (prephenate dehydrogenase and aromatic-amino-acid transaminase of Phe/Tyr synthesis, and undescribed steps of Lys and Pro synthesis), and one enzyme of the pentose phosphate cycle (cytosolic ribose 5-phosphate isomerase; Fig. 1, Fig. 2). Some of these steps are possibly catalyzed by distantly related enzymes that were not recognized by our searches, but other absences may be of biological relevance. Ribose 5-phosphate isomerase is necessary to recycle ribulose 5-phosphate, but a cytosolic isoform was not recovered, and maybe alternatively spliced transcripts encode for a truncated, non-plastid-targeted protein. Similarly, the final steps of fucoxanthin biosynthesis are missing. Although there are biochemical data that *Chromera* and *Vitrella*, respectively, accumulate (iso)fucoxanthin and vaucheriaxanthin – both derivates of neoxanthin – as accessory photosynthetic pigments (Moore et al. 2008; Oborník et al. 2012), neoxanthin synthase was not found in our data, while the

bioRxiv preprint doi: https://doi.org/10.1101/603555; this version posted April 9, 2019. The copyright holder for this preprint (which was not certified by peer review) is the author/funder, who has granted bioRxiv a license to display the preprint in perpetuity. It is made available under aCC-BY-NC-ND 4.0 International license.

last enzymes of the respective pathways are unknown (Mikami & Hosokawa 2013). In comparison, the absence of acyl-ACP synthase might be compensated if fatty acids are not released from the bond with the ACP but rather directly used for lipid synthesis (Bisanz et al. 2006). Alternatively, intermediate glycerolipids (diacylglycerol esterified with fatty acids of various length and saturation) could be imported from other cell compartments (Jouhet et al. 2007).

[insert Fig. 2]

Prediction performance

ASAFind and HECTAR (Gruber et al. 2015; Gschloessl et al. 2008) were designed to predict the BTS of plastid proteins in complex algae, particularly in heterokonts. ASAFind identifies plastid proteins based on the output of SignalP (Petersen et al. 2011) and a sliding-window scan for the highly conserved Phe residue around the predicted cleavage site. HECTAR uses a combination of predictors in three decision modules and aims to classify proteins based on presence of four types of targeting modules: signal peptides, type II signal anchors, chloroplast transit peptides, and mitochondrial transit peptides. To predict the mTP, several predictors are available. These include TargetP, MultiLoc2, and HECTAR (Emanuelsson et al. 2000; Blum et al. 2009; Gschloessl et al. 2008).

Both ASAFind and HECTAR were specifically trained on stramenopile sequences, though ASAFind offers the possibility to use an alternative bit score matrix derived from a training set. TargetP and MultiLoc2 were trained using plant and animal sequences. Having reference dataset at hand, we could test the performance of these algorithms on chromerid datasets, which has been unknown. Our results are summarized in Table 1 (full results in Supplementary Table S2). Mitochondrial predictors offered only

bioRxiv preprint doi: https://doi.org/10.1101/603555; this version posted April 9, 2019. The copyright holder for this preprint (which was not certified by peer review) is the author/funder, who has granted bioRxiv a license to display the preprint in perpetuity. It is made available under aCC-BY-NC-ND 4.0 International license.

moderate sensitivity and precision, with *V. brassicaformis* sequences being better resolved. We defined two thresholds for each predictor, one having higher sensitivity (around 75 %), the other more selective (with around 85 % precision). HECTAR offers higher precision with the 75%-level sensitivity compared to other mitochondrial predictors (Supplementary Fig. S3). With plastid sequences, ASAFind and HECTAR performed comparably, having both high sensitivity and precision. However, it must be noted that the threshold for HECTAR is very low and most of our plastid controls were marked as "secretory proteins" by this predictor. Our datasets might be over-fit by lacking enough endomembrane system proteins as negative controls, therefore precision is expected to drop with broader reference sets. We also used our plastid references to derive bit score-weighted matrices of amino acids flanking the cleavage site independently for *C. velia* and *V. brassicaformis* (as in Gruber et al. 2015). Using this matrix, we could further improve the performance of ASAFind (Table 1). This suggests that indeed chromerid plastid-targeting presequences differ from those of stramenopiles, but possibly also from each other.

[insert Table 1]

To visualize the amino acid enrichment around the signal cleavage site, we created logo-plots of amino acid frequencies in this motif in chromerids. We found that *C. velia* has a conserved Phe residue just after the cleavage site, which is not the case in *V. brassicaformis* that, instead, has a highly conserved Ala before the cleavage site (Fig. 3). Given that we used mostly orthologous sequences to create our datasets, we conclude that chromerids likely differ in the mechanisms that allow transit peptide recognition post import into ER, though the molecular basis of this alteration is currently unknown.

[insert Fig. 3]

bioRxiv preprint doi: https://doi.org/10.1101/603555; this version posted April 9, 2019. The copyright holder for this preprint (which was not certified by peer review) is the author/funder, who has granted bioRxiv a license to display the preprint in perpetuity. It is made available under aCC-BY-NC-ND 4.0 International license.

Plastid housekeeping

Most of the enzymes we expected to localize in chromerid plastids are directly or indirectly related to photosynthesis. These include the photosystems core subunits, the proteins of light-harvesting antennae and the photosynthetic electron transport chain, but also insertase proteins TAT, SEC and SRP/Alb3 that embed these factors in the thylakoid membrane (Fig. 2, discussed in further detail by Sobotka et al. 2017). Furthermore, we detected the many enzymatic steps that produce photosystems cofactors and accessory pigments (Fig. 1). Tetrapyrrole synthesis is one of the prime biochemical pathways of plastids, since heme is a vital component to the electron transport chain and retrograde plastid signaling, while chlorophyll is a fundamental cofactor in light harvesting complexes (de Souza et al., 2017). In *C. velia*, the tetrapyrrole pathway starts curiously with the delta-aminolevulinic acid (ALA) synthesis from glycine and succinyl-CoA in the mitochondrion, but the rest of the pathway is predicted to reside in the plastid (Kořený et al. 2011). This feature is shared by *V. brassicaformis* and indeed supported by our results (Fig. 1). Heme is also required for the function of cytosolic and mitochondrial hemoproteins (e.g., respiratory chain components), so it is exported from the chromerid plastid, as there is apparently no tetrapyrrole synthesis activity in other compartments besides ALA synthesis.

Chlorophyll *a* (Chl *a*) is the only chlorophyll species employed by chromerids (Moore et al. 2008). During the last step of Chl *a* synthesis, a terpenoid (phytyl) moiety is attached to the Mg^{2+}-coordinated tetrapyrrole, chlorophyllide *a*. Phytyl diphosphate is synthesized from methyl-D-erythritol 4-phosphate (MEP) and the pathway also resides in the chromerid plastid. The alternative cytosolic (mevalonate) pathway for terpenoid biosynthesis is missing, but terpenoid diphosphates are apparently exported from the

bioRxiv preprint doi: https://doi.org/10.1101/603555; this version posted April 9, 2019. The copyright holder for this preprint (which was not certified by peer review) is the author/funder, who has granted bioRxiv a license to display the preprint in perpetuity. It is made available under aCC-BY-NC-ND 4.0 International license.

plastid for further elongation by cytosolic and mitochondrial polyprenyl diphosphate synthases to produce, among others, ubiquinone for the mitochondrial respiratory chain (Supplementary Table S1, Supplementary Data S4; Imlay & Odom 2014).

Terpenoid derivatives include carotenoids and terpenoid quinones. Carotenoids violaxanthin and (iso)fucoxanthin are accessory photosynthetic pigments involved in light-harvesting, and the de-epoxidation of violaxanthin was suggested to be fundamental for photoprotection in *C. velia* (Kotabová et al. 2011). Plastoquinol is an electron transport chain electron mediator, while tocopherol has a protective role in oxidative stress (Müller & Kappes 2007). The plastid localization of these pathways therefore conditions the photosynthetic abilities of chromerids.

Fatty acid and lipid synthesis are important for the generation of plastid membranes and the modulation of their physicochemical properties. Chromerid plastids house the type II fatty acid synthesis pathway that is fed with acetyl-CoA by the plastid pyruvate dehydrogenase complex (Foth et al. 2005). The produced acyl-ACP molecules are then directly esterified with glycerol 3-phosphate to become intermediates of glycerolipid synthesis or are exported from the plastid and subject to elongation and desaturation (not shown, Tomčala et al., unpublished). Galactolipids of the mono- and digalactosyl-diacylglycerolipid groups (MGDG and DGDG) are major lipids of plastids in *C. velia* (Botté et al. 2011), required for proper embedding of photosystems into the thylakoid membranes but possibly also involved in plastid protein translocation (Schleiff et al. 2003). Their biosynthesis is limited to plastids in both *C. velia* and *V. brassicaformis*, as the respective protein contain plastid-targeting presequences (Fig. 1).

Flavin cofactors are critical for multiple enzymes of the TCA cycle, fatty acid oxidation, photosynthesis, respiratory chain, and *de novo* pyrimidine biosynthesis. In chromerids, riboflavin is synthesized in the plastid from a Calvin cycle intermediate,

bioRxiv preprint doi: https://doi.org/10.1101/603555; this version posted April 9, 2019. The copyright holder for this preprint (which was not certified by peer review) is the author/funder, who has granted bioRxiv a license to display the preprint in perpetuity. It is made available under aCC-BY-NC-ND 4.0 International license.

ribulose 5-phosphate, and flavin nucleotides are then supposedly exported from the plastid (Fig. 2).

Iron-sulfur clusters are components of redox proteins and in plastids, they function as the prosthetic group of the cytochrome b_6f and the ferredoxin redox relay that signals the plastid redox state to downstream enzymes. Plastid iron-sulfur clusters are typically synthesized by the SUF system, using ferrous ions and cysteine-derived sulfur as substrates. Both Cys synthesis and SUF system are found in chromerid plastids (Fig. 1), suggesting that plastid client proteins have regular access to Fe-S clusters.

Unexpectedly, only few enzymes of amino acid biosynthesis localize to plastids in *C. velia* and *V. brassicaformis*. We could reliably predict that only three enzymes of Cys synthesis reside in the plastid, but this amino acid is directly metabolized by the SUF system to assemble Fe-S clusters. Strikingly, plant chloroplasts synthesize several amino acids (Lys, Arg, Ala, Trp, Tyr, Phe; Van Dingenen et al. 2016) and participate on nitrogen assimilation with the glutamine synthase / glutamine oxoglutarate aminotransferase (GS/GOGAT) cycle. Apparently, chromerid plastids are much less involved in nitrogen metabolism than previously studied systems (see below).

In summary, chromerid plastids are well-equipped for the biogenesis and maintenance of the photosynthetic machinery. In addition, these organelles prime fatty acid and terpenoid biosynthesis by the formation of short-chain intermediates (short-chain saturated fatty acids and monoterpenoid diphosphates), that are however exported for further processing. Heme is another crucial compound produced in this compartment. All these processes seem closely coupled to photosynthesis and, importantly, to carbon fixation by the Calvin cycle, which will be overviewed in the next section.

bioRxiv preprint doi: https://doi.org/10.1101/603555; this version posted April 9, 2019. The copyright holder for this preprint (which was not certified by peer review) is the author/funder, who has granted bioRxiv a license to display the preprint in perpetuity. It is made available under aCC-BY-NC-ND 4.0 International license.

Compartment interplay

Calvin cycle is the very center of the second phase of photosynthesis; it utilizes ATP and NADPH produced by the light-dependent reactions to fix carbon dioxide into carbohydrates. We identified in chromerids all the enzymes of the cycle, discriminating them from the cytosolic carbohydrate metabolism variants by their N-terminal extensions having BTS characteristics. For three molecules of CO_2, the Calvin cycle produces one triose phosphate molecule (dihydroxyacetone phosphate – DHAP, or 3-phosphoglycerate) that can be metabolized by other pathways (see above), exported to the cytosol or reintroduced to the cycle to produce sugar phosphates with more carbons.

Triose phosphates enter the cytosol via the triose phosphate transporters, and those identified in *Plasmodium falciparum* prefer DHAP and phospho*enol*pyruvate (PEP) as substrates, while also accepting 3-phosphoglycerate (Lim et al. 2010). Upon the entry of triose phosphates to the cytosol, they can take two major paths, depending on the metabolic state. Gluconeogenetic pathway leads to the accumulation of storage saccharides (amylopectin), while glycolysis yields pyruvate, a hub compound for both anabolic and catabolic reactions. Generally, favorable and illuminated growth of algae promote storage and anabolic pathways, while dark growth and starvation promote spending of sugar phosphates in the TCA cycle and respiration.

We found enzymes involved in all processes of polysaccharide accumulation and degradation (Coppin et al. 2005). Some of the storage sugar enzymes encode signal peptides or transmembrane domains, suggestive of their extracellular or membrane-associated activity. This is consistent with chromerids forming a thick cellulose cell-wall (Moore et al. 2008; Oborník et al. 2012; Füssy & Oborník 2017a).

The Calvin cycle is not only a source of triose phosphates for cytosolic glycolysis/gluconeogenesis, but also of pentose phosphates that are the starting

bioRxiv preprint doi: https://doi.org/10.1101/603555; this version posted April 9, 2019. The copyright holder for this preprint (which was not certified by peer review) is the author/funder, who has granted bioRxiv a license to display the preprint in perpetuity. It is made available under aCC-BY-NC-ND 4.0 International license.

358 substrates for nucleotide (ribose 5-phosphate), amino acid (ribose 5-phosphate and
359 erythrose 4-phosphate), and vitamin synthesis (ribulose 5-phosphate). In this respect it
360 complements the cytosolic pentose phosphate cycle that also provides these sugar
361 phosphates. Based on our predictions, the plastid ribulose 5-phosphate pool serves as
362 the substrate for flavin nucleotide synthesis, while cytosolic ribulose 5-phosphate is
363 used for pyridoxin synthesis. Notably, we could not find any cytosolic 5-phosphoribosyl-
364 1-pyrophosphate (PRPP) synthases that would provide PRPP for the synthesis of His,
365 Trp and nucleotides in this compartment. Two pairs of orthologs are found in
366 chromerids. Each of these sequences has a presequence, though only two orthologs have
367 BTS (the other pair have mTP-like N-termini and were discarded from predictions due
368 to uncertain localization; Supplementary Table S1). Comparison with PRPP synthase
369 sequences from apicomplexans revealed that some of those too have predicted
370 presequences (including both *Toxoplasma gondii* ME49 paralogs), but proteins having
371 these presequences do not cluster together (Supplementary Data S4). The localization of
372 PRPP synthases is therefore questionable and might be achieved by alternative splicing.

373 Other anabolic reactions also stem from the cytosolic pool of sugar phosphates.
374 Biosynthesis of most amino acids in chromerids depends on glycolysis and pentose
375 phosphate cycle intermediates. Cys, Met and Ser derive from 3-phosphoglycerate, while
376 Phe, Trp and Tyr are synthesized from erythrose 4-phosphate via chorismate, and His is
377 a derivative of PRPP (but see above). Ala, Arg, Asp, Asn, Lys, Pro and Thr derive from 2-
378 oxoglutarate (2-OG) transaminated to form Glu by the GS/GOGAT cycle (Fig. 2). Notably,
379 the cytosolic 2-OG pool for GS/GOGAT cycle exists by the action of cytosolic copies of
380 TCA cycle enzymes (Fig. 2, Supplementary Table S1). Chromerid plastids do not
381 principally participate in the amino acid biosynthesis, with a few exceptions. A part of
382 the Arg pathway (ornithine synthesis) is predicted to localize in the plastid, which might

bioRxiv preprint doi: https://doi.org/10.1101/603555; this version posted April 9, 2019. The copyright holder for this preprint (which was not certified by peer review) is the author/funder, who has granted bioRxiv a license to display the preprint in perpetuity. It is made available under aCC-BY-NC-ND 4.0 International license.

be a rate-limiting, regulatory measure on ornithine production via dependence on stromal ATP levels. This is not unexpected, as in plants Arg synthesis is regulated at the level of N-acetylglutamine phosphorylation (Ferrario-Méry et al. 2006). Notably, chromerids utilize argJ (Supplementary Data S4), which is a glutamate transacetylating enzyme that allows to recycle N-acetylglutamate after the production of ornithine. This reaction does not produce free acetate and thus does not require additional ATP for acetyl-CoA recycling. In *Plasmodium*, *Cryptosporidium* and *Eimeria*, Arg (via ornithine) is used for polyamine synthesis (Cook et al. 2007) but this pathway shows cytosolic localization congruently in apicomplexans and chromerids (Supplementary Table S1; Shanmugasundram et al. 2013). Gly may be produced by glycine hydroxymethyltransferase and threonine aldolase in mitochondria, cytosol, and plastids (Supplementary Table S1), reflecting its involvement in multiple pathways as a reaction intermediate (for plastid formylmethionine and mitochondrial ALA synthesis, for instance). There is some incongruence about the localization of Ile, Leu and Val synthesis among chromerids, as *V. brassicaformis* appears to localize Val and Ile biosynthesis to both mitochondria and plastid while Leu biosynthesis is cytosolic. In comparison, all these pathway steps are cytosolic in *C. velia*. Chromerid plastids thus appear to have minor roles in amino acid biosynthesis.

Both catabolic and anabolic reactions were found to take place in the chromerid mitochondria, though they are missing some common components. Both apicomplexans and chromerids ancestrally lack the respiratory complex I (and *C. velia* also lacks complex III) and utilize alternative NADH dehydrogenases that pass electrons to ubiquinone but do not contribute to the proton gradient (Fig. 2, Flegontov et al. 2015). Like Apicomplexa, chromerids also lack a canonical mitochondrial pyruvate dehydrogenase and instead take advantage of the promiscuous activity of the branched-

bioRxiv preprint doi: https://doi.org/10.1101/603555; this version posted April 9, 2019. The copyright holder for this preprint (which was not certified by peer review) is the author/funder, who has granted bioRxiv a license to display the preprint in perpetuity. It is made available under aCC-BY-NC-ND 4.0 International license.

chain amino acid dehydrogenase (BKCDH) (Foth et al. 2005; Danne et al. 2013; Oppenheim et al. 2014). The NAD^+-dependent isocitrate dehydrogenase is missing and replaced by an $NADP^+$-dependent isozyme, which could be linked to the loss of the canonical NADH dehydrogenase (respiratory complex I). $NADP^+$-dependent isocitrate dehydrogenase might in turn support the activity of NADPH-dependent enzymes (Danne et al. 2013). This is notable because in mammals both NAD^+ and $NADP^+$ isocitrate dehydrogenases are operational, the latter typically in reverse (reductive) direction (Sazanov & Jackson 1994; Yoo et al. 2008). In contrast with apicomplexans, both fumarate hydratase types are present in chromerids (apicomplexans express only type I; Bulusu et al. 2011), while an ortholog of the conserved apicomplexan malate:quinone oxidoreductase is missing (Danne et al. 2013). Chromerids localize to mitochondria several enzymes of amino acid decomposition (Supplementary Table S1), suggesting that at least some catabolic pathways feed into the mitochondrial metabolism. A set of lactate dehydrogenases in chromerids may help them survive temporary dark anaerobic conditions via fermentation of pyruvate to lactate (Flegontov et al. 2015; Oborník & Lukeš 2015) and participate in methylglyoxal detoxication (Cordeiro et al. 2012). Furthermore, the mitochondrial metabolism is equipped with malic enzyme (decarboxylating malate dehydrogenase), which allows the regeneration of pyruvate for anabolic reactions when the cycle is fed by fatty acid beta-oxidation. Therefore, mitochondria are well-integrated in the chromerid carbon metabolism in both catabolic and anabolic directions.

Carbon metabolism also affects the synthesis rates of nitrogen pathways. The GS/GOGAT cycle is responsible for nitrogen (ammonia) assimilation into amino acids in most phototrophs. In chromerids, GOGAT is an NADH-dependent cytosolic enzyme, and the restriction of amino acid pathways to the cytosol suggests that they are decoupled

bioRxiv preprint doi: https://doi.org/10.1101/603555; this version posted April 9, 2019. The copyright holder for this preprint (which was not certified by peer review) is the author/funder, who has granted bioRxiv a license to display the preprint in perpetuity. It is made available under aCC-BY-NC-ND 4.0 International license.

from the redox state of the plastid and rather reflect the redox state of the cytosol (Fig. 2). This also suggests that the plastids of chromerids are not as deeply involved in primary metabolism as the plastids of primary algae and plants by lacking the ability to synthesize amino acids and polysaccharides. Instead, plastid activity is crucial in lower carbohydrate and fatty acid metabolism and appears to be sensed indirectly, through the supply of triose phosphates. Under favorable conditions, the cytosol is fed with photosynthetic sugar phosphates, and reducing agents and ATP are produced by glycolysis. This promotes anabolic reactions that allow the accumulation of polysaccharides and production of amino acids and lipids. In the dark or under nutrient scarcity, the shortage of energy must be compensated by the reactions of the TCA cycle and respiration in mitochondria. Unfortunately, there are no published large-scale quantitative data suitable for tracing in more detail the metabolic flows through the described pathways.

DISCUSSION

For proper function, proteins in eukaryotic cells need to be correctly localized to cellular compartments. Various protein translocation systems recognize amino acid signals encoded within their cargo and albeit they are not always conserved on sequence level, many of these signals have typical characteristics (Emanuelsson et al. 2007; Patron & Waller 2007; Kunze & Berger 2015; Wiedemann & Pfanner 2017). Signal peptides and mTPs guide proteins across the endoplasmic membrane and the mitochondrial envelope, respectively. The physicochemical character of these targeting presequences remains quite similar across long evolutionary distances among eukaryotes.

bioRxiv preprint doi: https://doi.org/10.1101/603555; this version posted April 9, 2019. The copyright holder for this preprint (which was not certified by peer review) is the author/funder, who has granted bioRxiv a license to display the preprint in perpetuity. It is made available under aCC-BY-NC-ND 4.0 International license.

Still, the predicting power of localization algorithms decreases with divergence between the reference and the analyzed sets. Prediction algorithms perform best if trained using lineage-specific datasets, usually based on available experimental data (e.g. (Emanuelsson et al. 2007; Kaundal et al. 2013; Gruber et al. 2015). Consistently, tools designed for primary algae and plants perform poorly with complex algal data (Patron & Waller 2007), as indeed the targeting presequences of primary and complex plastids differ notably due to the additional envelope membranes that enclose the latter. Similarly, lineages of complex algae arose from independent endosymbiotic events and so the plastid-localization signals show lineage-specific variability (Patron & Waller 2007). Although many tools have been implemented to determine mitochondrion- and plastid-localized proteins in *C. velia* and *V. brassicaformis* (Kořený et al. 2011; Woehle et al. 2011; Petersen et al. 2014; Flegontov et al. 2015; Woo et al. 2015; Sobotka et al. 2017), none of them have been tested on reference proteins in terms of predictive power. To find a suitable tool to predict protein localization in chromerids, we prepared a manually curated inventory of references that included proteins from plastid, mitochondrion, and several other compartments, as negative controls. To date, two works (Flegontov et al. 2015; Sobotka et al. 2017) have investigated the metabolism of chromerids on organellar level, and only the latter work supports the localization of analyzed (plastid) proteins with proteomic data. Our dataset included sequences of typical plastid-targeted proteins as well as proteins with unambiguous localization to mitochondria and other compartments, conserved in other eukaryotic lineages. To ensure that our sequences are largely complete at their N-termini, we used protein models generated by two independent sequencing initiatives, EuPathDB (deposited at CryptoDB; (Woo et al. 2015) and MMETSP (Keeling et al. 2014).

bioRxiv preprint doi: https://doi.org/10.1101/603555; this version posted April 9, 2019. The copyright holder for this preprint (which was not certified by peer review) is the author/funder, who has granted bioRxiv a license to display the preprint in perpetuity. It is made available under aCC-BY-NC-ND 4.0 International license.

We analyzed the performance of several algorithms based on their sensitivity (percentage of true positive sequences passing a threshold) and precision (percentage of false positives in the set passing the same threshold). For plastid proteomes, ASAFind using a species-specific bit score matrix was found to be the most efficient for each chromerid. The sensitivity of ASAFind with *Phaeodactylum tricornutum* sequences was comparable to our results (80%; Gruber et al. 2015). With mitochondrial references, we could not observe predictive differences for *V. brassicaformis* sequences. With *C. velia* datasets, HECTAR was more precise at higher sensitivity levels, and MultiLoc2 could not reach an 85% precision (Table 1). TargetP performed similarly to HECTAR (TargetP is indeed part of HECTAR's mitochondrial module) and is widely used for finding mitochondria-targeted genes with sensitivity around 60-75% (depending on the model and reliability class) in various organisms (Emanuelsson et al. 2007), including the chromerids (Kořený et al. 2011; Flegontov et al. 2015; Woo et al. 2015). This accuracy is also relatively lower because a portion of mitochondrial proteins use alternative routes or signals for translocation to this organelle (Sun & Habermann 2017). Several of our plastid and mitochondrial reference sequences were recovered as false negatives not passing the probability threshold. Indeed, 136 of the 1,141 reference sequences had alternative open reading frames or were unannotated and had to be manually adjusted using homology annotation, alignments and phylogenetic analyses (Supplementary Data S1). Importantly, we could find longer open reading frames for six paralogs of tetrapyrrole pathway enzymes published by Kořený et al. (2011), four of them with strong plastid presequences. Similarly, we could not obtain consistent localizations for the enzymes of the MEP pathway that is thought to be exclusively plastid-localized (Fig. 1). With untreated data, the false negative discovery rate would be much higher, leading to orphan enzymes predicted to unexpected compartments. This points out the

bioRxiv preprint doi: https://doi.org/10.1101/603555; this version posted April 9, 2019. The copyright holder for this preprint (which was not certified by peer review) is the author/funder, who has granted bioRxiv a license to display the preprint in perpetuity. It is made available under aCC-BY-NC-ND 4.0 International license.

problems with automated analyses – there is an essential need for highly complete sequence data, which worsens large-scale predictions in the chromerids.

Although targeting presequences are generally not generally not conserved on sequence level, the conservation of amino acids flanking the BTS cleavage sites was found to be crucial for proper plastid targeting (Gruber et al. 2007). Proteins targeted to the rhodophyte-derived complex plastids generally expose an invariant Phe at their N-terminus after signal peptide cleavage (Gould et al. 2006; Patron & Waller 2007). Based on our frequency matrices, in *Vitrella* plastid-targeted proteins the Phe motif is not strictly conserved, while most plastid-targeted proteins of *Chromera* do possess this Phe (Fig. 3). This suggests there is some versatility of the translocation machineries in chromerids. Indeed, the divergence between *C. velia* and *V. brassicaformis* is significant (Oborník et al. 2012; Oborník & Lukeš 2013; Füssy et al. 2017) and the differential retainment of the Phe motif is consistent with this observation. In addition, not all rhodophyte-derived lineages retain a high number of plastid-targeted proteins with the Phe; despite Phe occurs predominantly in cryptophytes (*Guillardia theta*) and heterokonts (*Thalassiosira pseudonana* and *Phaeodactylum tricornutum*), haptophytes apparently do not rely on Phe in their transit peptide presequences (Kilian & Kroth 2005; Patron & Waller 2007; Gruber et al. 2015). Phe motif is also absent from the transit peptides of chlorophyte-derived algae and from apicomplexans (Patron & Waller 2007).

The pathways that localize into plastids are typically associated with photosynthesis. We identified enzymes responsible for the synthesis of tetrapyrroles, terpenoids, carotenoids, lipids, iron-sulfur clusters and carbohydrates, hence compounds required for the proper assembly and function of the photosynthetic machinery. Our findings are consistent with previous biochemical analyses, showing

bioRxiv preprint doi: https://doi.org/10.1101/603555; this version posted April 9, 2019. The copyright holder for this preprint (which was not certified by peer review) is the author/funder, who has granted bioRxiv a license to display the preprint in perpetuity. It is made available under aCC-BY-NC-ND 4.0 International license.

that chromerids have a limited set of photosynthetic pigments (Moore et al. 2008; Kotabová et al. 2011) and that they exhibit unique structural changes to the photosystems (Sobotka et al. 2017). We show that terpenoid and lipid pathways are primed with substrates produced by the plastid carbohydrate metabolism (DHAP, pyruvate, and PEP) and linked with the rate of carbon fixation by substrate availability (Fig. 1). This is not unprecedented, as plant chloroplasts show a similar arrangement in photosynthetically active and inactive plastids (e.g. Neuhaus and Emes 2000).

Nevertheless, plastid products might be essential beyond photosynthesis, which is best illustrated by comparison of algae with relatives that lost photosynthetic abilities (e.g., Hadariová et al. 2018). Indeed, the biology of non-photosynthetic plastids has been best studied in apicomplexans to find suitable weak-spots of these infamous parasites. The apicoplast produces fatty acids and terpenoids and participates in heme synthesis to sustain parasite growth in hosts where salvage of these compounds is not possible (reviewed by van Dooren and Striepen 2013). This dependence on a remnant plastid can be regarded as an evolutionary constraint that cannot be easily overcome once parallel pathways in the cytosol or mitochondria are lost (though losses of plastids occasionally happen, see Füssy & Oborník 2018; Oborník 2018). Consistent with this view, apicomplexans lack apicoplast-independent pathways for terpenoid (via mevalonate), fatty acid (using type I fatty acid synthase, or FASI) and tetrapyrrole synthesis. Some apicomplexans appear to possess FASI-like enzymes, though functional analyses suggest that *Cryptosporidum* FASI is not involved in *de novo* fatty acid synthesis and rather accepts long-chain fatty acyl thioesters as substrates for elongation (Zhu et al. 2004). The importance of *Toxoplasma* FASI remains unclear, while other apicomplexan FASI-like enzymes might be involved in polyketide synthesis (Kohli et al. 2016).

bioRxiv preprint doi: https://doi.org/10.1101/603555; this version posted April 9, 2019. The copyright holder for this preprint (which was not certified by peer review) is the author/funder, who has granted bioRxiv a license to display the preprint in perpetuity. It is made available under aCC-BY-NC-ND 4.0 International license.

The photosynthetic relatives to apicomplexans, chromerids are also likely to lack cytosolic pathways for fatty acid, terpenoid and tetrapyrrole synthesis and thus rely entirely on the plastid synthesis. In addition, chromerid plastids synthesize FAD cofactors and a nitrogen metabolism intermediate, ornithine (see below). Conversely, chromerid plastids do not host any fatty acid elongases or desaturases, therefore short-chain fatty acids need to be exported, processed and reimported for incorporation into plastid glycerolipids (Tomčala et al., unpublished), as these mostly contain long-chain, (poly)unsaturated fatty acids (Botté et al. 2011). This is analogous to the fatty acid synthesis architecture in apicomplexans (Mazumdar & Striepen 2007). Similarly, chromerid tetrapyrrole biosynthesis relies on the import of the starting substrate, ALA, from the cytosol (Kořený et al. 2011). Therefore, chromerid plastids pathways are interdependent with the cytosol, pointing out possible feedback regulatory mechanisms to limit their biosynthetic activity.

Under favorable conditions, the plastids of chromerids provide triose phosphates as the most important photosynthate. Once channeled to the cytosol via triose phosphate transporters (Lim et al. 2010), the pool of triose phosphates is used for storage sugar synthesis, but also various other anabolic reactions, such as amino acid, nucleotide and vitamin synthesis. In the dark, the reduced triose phosphate supply from the chromerid plastid must be counterbalanced by catabolic reactions of the mitochondrial TCA cycle and respiration. The chromerid TCA cycle and respiratory chain represent modifications to the canonical mitochondrial pathways, with changes including the functional replacement of pyruvate dehydrogenase by branched-chain amino acid dehydrogenase, replacement of NAD^+-dependent isocitrate dehydrogenase by $NADP^+$ isozyme, loss of respiratory chain complex(es) and enrichment in lactate dehydrogenases (see Results). The list of chromerid mitochondrial enzymes is largely

bioRxiv preprint doi: https://doi.org/10.1101/603555; this version posted April 9, 2019. The copyright holder for this preprint (which was not certified by peer review) is the author/funder, who has granted bioRxiv a license to display the preprint in perpetuity. It is made available under aCC-BY-NC-ND 4.0 International license.

shared with parasitic apicomplexans (Flegontov et al. 2015; Jacot et al. 2016). As yet, it is unclear what impact this arrangement has on the metabolism of photoautotrophic organisms, but it stands out that through the TCA cycle chromerid mitochondria are metabolically versatile and integrate catabolic pathways with enzymes priming anabolic reactions and enzymes typically associated with anaerobiosis (Flegontov et al. 2015). Notably, purine salvage from oxaloacetate is vital for *Plasmodium*, while the importance of the TCA cycle is diminished in asexual stages that thrive on glucose obtained from the host (Bulusu et al. 2011; Ke et al. 2015). Similarly, cytosolic ATP citrate lyase contributes to acetyl-CoA production in *T. gondii* (Tymoshenko et al. 2015). As such, chromerid mitochondria are likely to have major influence on metabolic fluxes in the cell.

We observed that amino acid biosynthesis pathways consistently showed cytosolic localizations, with minor exceptions. This is probably not due to misannotation as we could not extend the sequences towards an alternative N-terminus in most cases. Chromerid plastids thus appear to host only parts of Cys and Arg synthesis, suggesting that amino acids are not necessarily synthesized in plastids as in plants (Van Dingenen et al. 2016). While plastid Cys synthesis is required by the Fe-S cluster assembly system SUF, the plastid production of ornithine for Arg biosynthesis might have a regulatory role in chromerids. Indeed, nitrogen metabolism is energy-demanding and subject to intense cross-talk with carbon metabolism, and plastids play a crucial role in balancing the fluxes (Stitt 2002; Németh et al. 2018). As yet, the primarily cytosolic localization of nitrogen metabolism in chromerids appears extraordinary among phototrophs (Allen et al. 2011; Bromke 2013; de la Torre et al. 2013; Dorrell et al. 2017). Of studied apicomplexans, *Toxoplasma* has the broadest capacity to produce amino acids *de novo* or secondarily from specific precursors, being auxotrophic only for Arg, His and Trp (Chaudhary et al. 2014; Tymoshenko et al. 2015). Although the middle steps of Pro and

bioRxiv preprint doi: https://doi.org/10.1101/603555; this version posted April 9, 2019. The copyright holder for this preprint (which was not certified by peer review) is the author/funder, who has granted bioRxiv a license to display the preprint in perpetuity. It is made available under aCC-BY-NC-ND 4.0 International license.

Lys synthesis are currently unknown (Shanmugasundram et al. 2013), none of these amino acid synthesis pathways appears to be placed exclusively in the apicoplast, in line with our results. Arg scavenging from outer sources might have therefore triggered the loss of the ornithine cycle in the ancestor of apicomplexans. Reliance on amino acid import from the host resulted in even greater reduction of amino acid synthesis capabilities. Thus, *Plasmodium* synthesizes six amino acids (Gly, Glu, Gln, Pro, Asp, Asn), while *Cryptosporidium,* which entirely lacks an apicoplast (Keithly et al. 2000; Chaudhary et al. 2014), synthesizes only Gly, Glu and Pro. It is tempting to speculate that the major role of the cytosol in amino acid synthesis facilitated the plastid loss in a distantly related non-photosynthetic dinoflagellate, *Hematodinium* (Gornik et al. 2015).

In apicomplexans, indeed, the main source of energy is glycolysis of host-drawn glucose, but the parasites appear to use the same carbohydrate subpathways as chromerids. These include the compartment exchange of triose phosphates via phosphate transporters (Lim et al. 2010), parallel cytosolic and plastid glycolysis to pyruvate (Fleige et al. 2007), cytosolic accumulation of storage polysaccharides (Coppin et al. 2005) and a notable relocation of the canonical pyruvate dehydrogenase in the apicoplast to feed the fatty acid synthesis (Foth et al. 2005; Fleige et al. 2007). There are also obvious commonalities in the arrangement of mitochondrial metabolism, including the modifications of the canonical TCA cycle, the respiratory chain, and the anabolic reactions of mitochondria. As this arrangement is largely shared among chromerids and apicomplexans, it likely represents an ancestral state employed the phototrophic progenitor of both groups.

The overall architecture of biosynthetic pathways in chromerids suggests that their cytosol represents the compartment which integrates the cellular energy status based on photosynthate supply from the plastid and nutrient availability. Through

bioRxiv preprint doi: https://doi.org/10.1101/603555; this version posted April 9, 2019. The copyright holder for this preprint (which was not certified by peer review) is the author/funder, who has granted bioRxiv a license to display the preprint in perpetuity. It is made available under aCC-BY-NC-ND 4.0 International license.

metabolite flow it can directly regulate energy storage accumulation and the biosynthesis of lipids, nucleotides, amino acids and other vital biomolecules, or redirect carbon compounds to mitochondria to produce energy more efficiently via the respiratory chain when photosynthate supply is short. Hypothetically, such a central role for the cytosol could have been employed by a free-living unicellular eukaryovore/algivore that ingests its prey into a food vacuole and gradually digests it, much like the one we picture was the ancestor of Myzozoa (Tikhonenkov et al. 2014). Indeed, the broad spectrum of apicomplexan cell-surface transporters raises the question whether chromerids also take advantage of extracellular sources of a comparable number of organic molecules. Indeed, both chromerids were isolated as coral-associated organisms (Moore et al. 2008; Oborník et al. 2012) and intriguing data have been presented on mixotrophy of *C. velia* and its association with corals (Cumbo et al. 2013; Foster et al. 2014; Mohamed et al. 2018). This question therefore needs to be addressed in more detail, as it might present implications on the early evolution of apicomplexans themselves. However, experimental data are currently unavailable to present an in-depth metabolomic model for chromerids and we can merely compare our results with those from apicomplexans. Here we present a benchmark set of biochemical pathways that can be investigated by quantitative or phylogenetic approaches for a deeper understanding of the "alveolate way" of trophic transition from photosynthetic algae to obligatory parasites.

CONCLUSIONS

Chromerids occupy a pivotal position in the tree of alveolates and hold the key to our understanding of transition to parasitism; they are free-living phototrophic algae

bioRxiv preprint doi: https://doi.org/10.1101/603555; this version posted April 9, 2019. The copyright holder for this preprint (which was not certified by peer review) is the author/funder, who has granted bioRxiv a license to display the preprint in perpetuity. It is made available under aCC-BY-NC-ND 4.0 International license.

with relatively canonical chromosomes and branch sister to the apicomplexans. To sketch a few more pathways on the metabolic map of chromerids, we prepared reference datasets of plastid, cytosolic and mitochondrial enzymes. We have manually curated these protein sequences so that most of them are complete, which is crucial for correct predictions of their subcellular localization. We unveiled that chromerid plastids vividly exchange compounds with the cytosol and mitochondria in order to produce terpenoids, lipids and tetrapyrroles. In contrast, chromerid plastids appear to have only a minor role in amino acid synthesis, as most of these pathways reside in the cytosol. Uniquely, chromerids were found to use a plastid ornithine cycle combined with a cytosolic Arg cycle for synthesis and decomposition of this amino acid. We outlined a major hub represented by lower glycolysis and gluconeogenesis enzymes that appears to regulate carbon and nitrogen metabolite flow depending on the photoactivity of the plastid. We compared our model to apicomplexan metabolic pathways and saw a conserved architecture of carbon and nitrogen metabolism in these groups. Further analyses are though needed to gain insight into the regulation of these pathways in response to various cues. Using the suggested prediction tools, it is now also possible to introduce more enzymatic steps to the picture.

ABBREVIATIONS: 2-OG – 2-oxoglutarate, ACP – acyl-carrier protein, ALA – delta-aminolevulinic acid, BTS – bipartite (plastid) targeting signal, Chl *a* – chlorophyll *a*, DGDG/MGDG – di-/monogalactosyl-diacylglycerolipid, DHAP – dihydroxyacetone phosphate, Ery-4P – erythrose 4-phosphate, FAD – flavin adenine dinucleotide, GS/GOGAT – glutamine synthase / glutamine oxoglutarate aminotransferase, IMS – inter-membrane space, MEP – methyl-D-erythritol 4-phosphate, mTP – mitochondrial

bioRxiv preprint doi: https://doi.org/10.1101/603555; this version posted April 9, 2019. The copyright holder for this preprint (which was not certified by peer review) is the author/funder, who has granted bioRxiv a license to display the preprint in perpetuity. It is made available under aCC-BY-NC-ND 4.0 International license.

transit peptide, OAA – oxaloacetate, orn – ornithine, PEP – phospho*enol*pyruvate, PQ – plastoquinol, PRPP – 5-phosphoribosyl-1-pyrophosphate, pyr – pyruvate, Ru-5P – ribulose 5-phosphate, TCA – tricarboxylic acid, THF - tetrahydrofolate, UQ - ubiquinone.

ETHICS APPROVAL AND CONSENT TO PARTICIPATE

Not applicable.

CONSENT FOR PUBLICATION

Not applicable.

COMPETING INTEREST

The authors declare that they have no competing interests.

AUTHORS' CONTRIBUTIONS

MO and ZF conceived the study. ZF and TF performed all the bioinformatic analyses and prepared the figures and tables. ZF drafted the manuscript. MO acquired funding. All authors edited the manuscript and approved its final form.

ACKNOWLEDGEMENTS

The authors would like to thank the Czech Science Foundation (project 16-24027S granted to MO) and the European Regional Development Fund (ERDF) (No. CZ.02.1.01/0.0/0.0/16_019/0000759) for funding. Computational resources from MetaCentrum and CERIT-SC, Brno, Czech Republic, are greatly appreciated. We are grateful to Ansgar Gruber for helpful discussions.

bioRxiv preprint doi: https://doi.org/10.1101/603555; this version posted April 9, 2019. The copyright holder for this preprint (which was not certified by peer review) is the author/funder, who has granted bioRxiv a license to display the preprint in perpetuity. It is made available under aCC-BY-NC-ND 4.0 International license.

REFERENCES

Allen AE et al. 2011. Evolution and metabolic significance of the urea cycle in photosynthetic diatoms. Nature. 473:203–207. doi: 10.1038/nature10074.

Atteia A et al. 2009. A proteomic survey of *Chlamydomonas reinhardtii* mitochondria sheds new light on the metabolic plasticity of the organelle and on the nature of the α-proteobacterial mitochondrial ancestor. Mol. Biol. Evol. 26:1533–1548. doi: 10.1093/molbev/msp068.

Bisanz C et al. 2006. *Toxoplasma gondii* acyl-lipid metabolism: *de novo* synthesis from apicoplast-generated fatty acids versus scavenging of host cell precursors. Biochem. J. 394:197–205. doi: 10.1042/BJ20050609.

Blum T, Briesemeister S, Kohlbacher O. 2009. MultiLoc2: Integrating phylogeny and Gene Ontology terms improves subcellular protein localization prediction. BMC Bioinformatics. 10:274. doi: 10.1186/1471-2105-10-274.

Botté CY et al. 2011. Identification of plant-like galactolipids in *Chromera velia*, a photosynthetic relative of malaria parasites. J. Biol. Chem. 286:29893–29903. doi: 10.1074/jbc.M111.254979.

Boucher MJ et al. 2018. Integrative proteomics and bioinformatic prediction enable a high-confidence apicoplast proteome in malaria parasites. PLoS Biol. 16:1–29. doi: 10.1371/journal.pbio.2005895.

Bromke MA. 2013. Amino acid biosynthesis pathways in diatoms. Metabolites. 3:294–311. doi: 10.3390/metabo3020294.

Buchfink B, Xie C, Huson DH. 2014. Fast and sensitive protein alignment using DIAMOND. Nat. Methods. 12:59. doi: 10.1038/nmeth.3176.

bioRxiv preprint doi: https://doi.org/10.1101/603555; this version posted April 9, 2019. The copyright holder for this preprint (which was not certified by peer review) is the author/funder, who has granted bioRxiv a license to display the preprint in perpetuity. It is made available under aCC-BY-NC-ND 4.0 International license.

Bulusu V, Jayaraman V, Balaram H. 2011. Metabolic fate of fumarate, a side product of the purine salvage pathway in the intraerythrocytic stages of *Plasmodium falciparum*. J. Biol. Chem. 286:9236–9245. doi: 10.1074/jbc.M110.173328.

Burki F et al. 2012. Re-evaluating the green versus red signal in eukaryotes with secondary plastid of red algal origin. Genome Biol. Evol. 4:626–635. doi: 10.1093/gbe/evs049.

Calvo SE, Mootha VK. 2010. The mitochondrial proteome and human disease. Annu. Rev. Genomics Hum. Genet. 11:25–44. doi: 10.1146/annurev-genom-082509-141720.

Capella-Gutiérrez S, Silla-Martínez JM, Gabaldón T. 2009. trimAl: A tool for automated alignment trimming in large-scale phylogenetic analyses. Bioinformatics. 25:1972–1973. doi: 10.1093/bioinformatics/btp348.

Chaudhary K, Fox BA, Bzik DJ. 2014. Comparative aspects of nucleotide and amino acid metabolism in *Toxoplasma gondii* and other Apicomplexa. In: Toxoplasma gondii (2nd Edition). Weiss, LM & Kim, K, editors. Elsevier pp. 663–706. doi: 10.1016/B978-0-12-396481-6.00020-9.

Cohen L, Alexander H, Brown CT. 2016. Marine Microbial Eukaryotic Transcriptome Sequencing Project, re-assemblies. figshare. 3840153.

Cook T et al. 2007. Divergent polyamine metabolism in the Apicomplexa. Microbiology. 153:1123–1130. doi: 10.1099/mic.0.2006/001768-0.

Coppin A et al. 2005. Evolution of plant-like crystalline storage polysaccharide in the protozoan parasite *Toxoplasma gondii* argues for a red alga ancestry. J. Mol. Evol. 60:257–267. doi: 10.1007/s00239-004-0185-6.

Cordeiro C et al. 2012. The glyoxalase pathway in protozoan parasites. Int. J. Med. Microbiol. 302:225–229. doi: 10.1016/j.ijmm.2012.07.005.

Crooks G, Hon G, Chandonia J, Brenner S. 2004. WebLogo: A sequence logo generator.

bioRxiv preprint doi: https://doi.org/10.1101/603555; this version posted April 9, 2019. The copyright holder for this preprint (which was not certified by peer review) is the author/funder, who has granted bioRxiv a license to display the preprint in perpetuity. It is made available under aCC-BY-NC-ND 4.0 International license.

Genome Res. 14:1188–1190. doi: 10.1101/gr.849004.1.

Cumbo VR et al. 2013. *Chromera velia* is endosymbiotic in larvae of the reef corals *Acropora digitifera* and *A. tenuis*. Protist. 164:237–244. doi: 10.1016/j.protis.2012.08.003.

Danne JC, Gornik SG, MacRae JI, McConville MJ, Waller RF. 2013. Alveolate mitochondrial metabolic evolution: Dinoflagellates force reassessment of the role of parasitism as a driver of change in apicomplexans. Mol. Biol. Evol. 30:123–139. doi: 10.1093/molbev/mss205.

Van Dingenen J, Blomme J, Gonzalez N, Inzé D. 2016. Plants grow with a little help from their organelle friends. J. Exp. Bot. 67:6267–6281. doi: 10.1093/jxb/erw399.

van Dooren GG, Striepen B. 2013. The algal past and parasite present of the apicoplast. Annu. Rev. Microbiol. 67:271–289. doi: 10.1146/annurev-micro-092412-155741.

Dorrell RG et al. 2017. Chimeric origins of ochrophytes and haptophytes revealed through an ancient plastid proteome. eLife. 6:e23717. doi: 10.7554/eLife.23717.

Dorrell RG, Butterfield ER, Nisbet RER, Howe CJ. 2013. Evolution: Unveiling early alveolates. Curr. Biol. 23:R1093–R1096. doi: 10.1016/j.cub.2013.10.055.

Dorrell RG, Drew J, Nisbet RER, Howe CJ. 2014. Evolution of chloroplast transcript processing in *Plasmodium* and its chromerid algal relatives Dutcher, SK, editor. PLoS Genet. 10:e1004008. doi: 10.1371/journal.pgen.1004008.

Emanuelsson O, Brunak S, von Heijne G, Nielsen H. 2007. Locating proteins in the cell using TargetP, SignalP and related tools. Nat. Protoc. 2:953–971. doi: 10.1038/nprot.2007.131.

Emanuelsson O, Nielsen H, Brunak S, Von Heijne G. 2000. Predicting subcellular localization of proteins based on their N-terminal amino acid sequence. J. Mol. Biol. 300:1005–1016. doi: 10.1006/jmbi.2000.3903.

bioRxiv preprint doi: https://doi.org/10.1101/603555; this version posted April 9, 2019. The copyright holder for this preprint (which was not certified by peer review) is the author/funder, who has granted bioRxiv a license to display the preprint in perpetuity. It is made available under aCC-BY-NC-ND 4.0 International license.

Ferrario-Méry S, Besin E, Pichon O, Meyer C, Hodges M. 2006. The regulatory PII protein controls arginine biosynthesis in *Arabidopsis*. FEBS Lett. 580:2015–2020. doi: 10.1016/j.febslet.2006.02.075.

Flegontov P et al. 2015. Divergent mitochondrial respiratory chains in phototrophic relatives of apicomplexan parasites. Mol. Biol. Evol. 32:1115–1131. doi: 10.1093/molbev/msv021.

Fleige T, Fischer K, Ferguson DJP, Gross U, Bohne W. 2007. Carbohydrate metabolism in the *Toxoplasma gondii* apicoplast: Localization of three glycolytic isoenzymes, the single pyruvate dehydrogenase complex, and a plastid phosphate translocator. Eukaryot. Cell. 6:984–996. doi: 10.1128/EC.00061-07.

Foster C, Portman N, Chen M, Šlapeta J. 2014. Increased growth and pigment content of *Chromera velia* in mixotrophic culture. FEMS Microbiol. Ecol. 88:121–128. doi: 10.1111/1574-6941.12275.

Foth BJ et al. 2005. The malaria parasite *Plasmodium falciparum* has only one pyruvate dehydrogenase complex, which is located in the apicoplast. Mol. Microbiol. 55:39–53. doi: 10.1111/j.1365-2958.2004.04407.x.

Füssy Z, Masařová P, Kručinská J, Esson HJHJ, Oborník M. 2017. Budding of the alveolate alga *Vitrella brassicaformis* resembles sexual and asexual processes in apicomplexan parasites. Protist. 168:80–91. doi: 10.1016/j.protis.2016.12.001.

Füssy Z, Oborník M. 2017a. Chromerids and their plastids. In: Advances in Botanical Research. Hirakawa, Y, editor. Vol. 84 pp. 187–218. doi: 10.1016/bs.abr.2017.07.001.

Füssy Z, Oborník M. 2018. Complex endosymbioses I: From primary to complex plastids, multiple independent events. Methods Mol. Biol. 1829:17–35. doi: 10.1007/978-1-4939-8654-5_2.

Füssy Z, Oborník M. 2017b. Reductive evolution of apicomplexan parasites from

bioRxiv preprint doi: https://doi.org/10.1101/603555; this version posted April 9, 2019. The copyright holder for this preprint (which was not certified by peer review) is the author/funder, who has granted bioRxiv a license to display the preprint in perpetuity. It is made available under aCC-BY-NC-ND 4.0 International license.

phototrophic ancestors. In: Evolutionary Biology: Self/Nonself Evolution, Species and Complex Traits Evolution, Methods and Concepts. Pontarotti, P, editor. Springer International Publishing: Cham pp. 217–236. doi: 10.1007/978-3-319-61569-1_12.

Garg SG, Gould SB. 2016. The role of charge in protein targeting evolution. Trends Cell Biol. 26:894–905. doi: 10.1016/j.tcb.2016.07.001.

Gawryluk RMR, Chisholm KA, Pinto DM, Gray MW. 2014. Compositional complexity of the mitochondrial proteome of a unicellular eukaryote (*Acanthamoeba castellanii*, supergroup Amoebozoa) rivals that of animals, fungi, and plants. J. Proteomics. 109:400–416. doi: 10.1016/j.jprot.2014.07.005.

Gonczarowska-Jorge H, Zahedi RP, Sickmann A. 2017. The proteome of baker's yeast mitochondria. Mitochondrion. 33:15–21. doi: 10.1016/j.mito.2016.08.007.

Gornik SG et al. 2015. Endosymbiosis undone by stepwise elimination of the plastid in a parasitic dinoflagellate. Proc. Natl. Acad. Sci. U. S. A. 112:5767–72. doi: 10.1073/pnas.1423400112.

Gould SB et al. 2006. Protein targeting into the complex plastid of cryptophytes. J. Mol. Evol. 62:674–681. doi: 10.1007/s00239-005-0099-y.

Gray MW. 2015. Mosaic nature of the mitochondrial proteome: Implications for the origin and evolution of mitochondria. Proc. Natl. Acad. Sci. U. S. A. 112:10133–8. doi: 10.1073/pnas.1421379112.

Gruber A et al. 2007. Protein targeting into complex diatom plastids: Functional characterisation of a specific targeting motif. Plant Mol. Biol. 64:519–530. doi: 10.1007/s11103-007-9171-x.

Gruber A. 2019. What's in a name? How organelles of endosymbiotic origin can be distinguished from endosymbionts. Microb. Cell. 6:123–133. doi: 10.15698/mic2019.02.668.

bioRxiv preprint doi: https://doi.org/10.1101/603555; this version posted April 9, 2019. The copyright holder for this preprint (which was not certified by peer review) is the author/funder, who has granted bioRxiv a license to display the preprint in perpetuity. It is made available under aCC-BY-NC-ND 4.0 International license.

Gruber A, Rocap G, Kroth PG, Armbrust EV, Mock T. 2015. Plastid proteome prediction for diatoms and other algae with secondary plastids of the red lineage. Plant J. 81:519–528. doi: 10.1111/tpj.12734.

Gschloessl B, Guermeur Y, Cock JM. 2008. HECTAR: A method to predict subcellular targeting in heterokonts. BMC Bioinformatics. 9:393. doi: 10.1186/1471-2105-9-393.

Gupta A et al. 2014. Reduced ribosomes of the apicoplast and mitochondrion of Plasmodium spp. and predicted interactions with antibiotics. Open Biol. 4:140045. doi: 10.1098/rsob.140045.

Hadariová L, Vesteg M, Hampl V, Krajčovič J. 2018. Reductive evolution of chloroplasts in non-photosynthetic plants, algae and protists. Curr. Genet. 64:365–387. doi: 10.1007/s00294-017-0761-0.

Hiller K, Grote A, Scheer M, Münch R, Jahn D. 2004. PrediSi: Prediction of signal peptides and their cleavage positions. Nucleic Acids Res. 32:375–379. doi: 10.1093/nar/gkh378.

Hopkins JF et al. 2012. Proteomics reveals plastid- and periplastid-targeted proteins in the chlorarachniophyte alga *Bigelowiella natans*. Genome Biol. Evol. 4:1391–1406. doi: 10.1093/gbe/evs115.

Huang S, Shingaki-Wells RN, Taylor NL, Millar AH. 2013. The rice mitochondria proteome and its response during development and to the environment. Front. Plant Sci. 4:16. doi: 10.3389/fpls.2013.00016.

Imlay L, Odom AR. 2014. Isoprenoid metabolism in apicomplexan parasites. Curr. Clin. Microbiol. Reports. 1:37–50. doi: 10.1007/s40588-014-0006-7.

Jacot D, Waller RF, Soldati-Favre D, MacPherson DA, MacRae JI. 2016. Apicomplexan energy metabolism: Carbon source promiscuity and the quiescence hyperbole. Trends Parasitol. 32:56–70. doi: 10.1016/j.pt.2015.09.001.

Janouškovec J et al. 2013. Colponemids represent multiple ancient alveolate lineages.

bioRxiv preprint doi: https://doi.org/10.1101/603555; this version posted April 9, 2019. The copyright holder for this preprint (which was not certified by peer review) is the author/funder, who has granted bioRxiv a license to display the preprint in perpetuity. It is made available under aCC-BY-NC-ND 4.0 International license.

Curr. Biol. 23:2546–2552. doi: 10.1016/j.cub.2013.10.062.

Janouškovec J et al. 2015. Factors mediating plastid dependency and the origins of parasitism in apicomplexans and their close relatives. Proc. Natl. Acad. Sci. 112:10200–10207. doi: 10.1073/pnas.1423790112.

Janouškovec J, Horák A, Oborník M, Lukeš J, Keeling PJ. 2010. A common red algal origin of the apicomplexan, dinoflagellate, and heterokont plastids. Proc. Natl. Acad. Sci. 107:10949–10954. doi: 10.1073/pnas.1003335107.

Jones P et al. 2014. InterProScan 5: genome-scale protein function classification. Bioinformatics. 30:1236–1240. doi: 10.1093/bioinformatics/btu031.

Jouhet J, Maréchal E, Block MA. 2007. Glycerolipid transfer for the building of membranes in plant cells. Prog. Lipid Res. 46:37–55. doi: 10.1016/j.plipres.2006.06.002.

Joy JB, Liang RH, McCloskey RM, Nguyen T, Poon AFY. 2016. Ancestral reconstruction. PLoS Comput. Biol. 12:e1004763. doi: 10.1371/journal.pcbi.1004763.

Kanehisa M, Furumichi M, Tanabe M, Sato Y, Morishima K. 2017. KEGG: new perspectives on genomes, pathways, diseases and drugs. Nucleic Acids Res. 45:D353–D361. doi: 10.1093/nar/gkw1092.

Katoh K, Standley DM. 2013. MAFFT multiple sequence alignment software version 7: Improvements in performance and usability. Mol. Biol. Evol. 30:772–780. doi: 10.1093/molbev/mst010.

Kaundal R, Sahu SS, Verma R, Weirick T. 2013. Identification and characterization of plastid-type proteins from sequence-attributed features using machine learning. BMC Bioinformatics. 14:S7. doi: 10.1186/1471-2105-14-S14-S7.

Ke H et al. 2015. Genetic investigation of tricarboxylic acid metabolism during the *Plasmodium falciparum* life cycle. Cell Rep. 11:164–174. doi: 10.1016/j.celrep.2015.03.011.

bioRxiv preprint doi: https://doi.org/10.1101/603555; this version posted April 9, 2019. The copyright holder for this preprint (which was not certified by peer review) is the author/funder, who has granted bioRxiv a license to display the preprint in perpetuity. It is made available under aCC-BY-NC-ND 4.0 International license.

Kearse M et al. 2012. Geneious Basic: An integrated and extendable desktop software platform for the organization and analysis of sequence data. Bioinformatics. 28:1647–1649. doi: 10.1093/bioinformatics/bts199.

Keeling PJ et al. 2014. The Marine Microbial Eukaryote Transcriptome Sequencing Project (MMETSP): Illuminating the functional diversity of eukaryotic life in the oceans through transcriptome sequencing. PLoS Biol. 12:e1001889. doi: 10.1371/journal.pbio.1001889.

Keithly JS, Marchewka MJ, Zhu G, Marchewka MJ, Keithly JS. 2000. *Cryptosporidium parvum* appears to lack a plastid genome. Microbiology. 146:315–321. doi: 10.1055/s-2001-18357.

Kersey PJ et al. 2016. Ensembl Genomes 2016: more genomes, more complexity. Nucleic Acids Res. 44:D574–D580. doi: 10.1093/nar/gkv1209.

Kilian O, Kroth PG. 2005. Identification and characterization of a new conserved motif within the presequence of proteins targeted into complex diatom plastids. Plant J. 41:175–183. doi: 10.1111/j.1365-313X.2004.02294.x.

Kohli GS, John U, Van Dolah FM, Murray SA. 2016. Evolutionary distinctiveness of fatty acid and polyketide synthesis in eukaryotes. ISME J. 10:1877–1890. doi: 10.1038/ismej.2015.263.

Kořený L, Sobotka R, Janouškovec J, Keeling PJ, Oborník M. 2011. Tetrapyrrole synthesis of photosynthetic chromerids is likely homologous to the unusual pathway of apicomplexan parasites. Plant Cell. 23:3454–3462. doi: 10.1105/tpc.111.089102.

Kotabová E, Kaňa R, Jarešová J, Prášil O. 2011. Non-photochemical fluorescence quenching in *Chromera velia* is enabled by fast violaxanthin de-epoxidation. FEBS Lett. 585:1941–1945. doi: 10.1016/j.febslet.2011.05.015.

Kunze M, Berger J. 2015. The similarity between N-terminal targeting signals for protein

bioRxiv preprint doi: https://doi.org/10.1101/603555; this version posted April 9, 2019. The copyright holder for this preprint (which was not certified by peer review) is the author/funder, who has granted bioRxiv a license to display the preprint in perpetuity. It is made available under aCC-BY-NC-ND 4.0 International license.

import into different organelles and its evolutionary relevance. Front. Physiol. 6:1–27. doi: 10.3389/fphys.2015.00259.

de la Torre F, El-Azaz J, Ávila C, Cánovas FM. 2013. Deciphering the role of aspartate and prephenate aminotransferase activities in plastid nitrogen metabolism. Plant Physiol. 164:92–104. doi: 10.1104/pp.113.232462.

Lim L, Linka M, Mullin KA, Weber APM, Mcfadden GI. 2010. The carbon and energy sources of the non-photosynthetic plastid in the malaria parasite. FEBS Lett. 584:549–554. doi: 10.1016/j.febslet.2009.11.097.

Mallo N, Fellows J, Johnson C, Sheiner L. 2018. Protein import into the endosymbiotic organelles of apicomplexan parasites. Genes (Basel). 9:412. doi: 10.3390/genes9080412.

Mazumdar J, Striepen B. 2007. Make it or take it: Fatty acid metabolism of apicomplexan parasites. Eukaryot. Cell. 6:1727–1735. doi: 10.1128/ec.00255-07.

Mikami K, Hosokawa M. 2013. Biosynthetic pathway and health benefits of fucoxanthin, an algae-specific xanthophyll in brown seaweeds. Int. J. Mol. Sci. 14:13763–13781. doi: 10.3390/ijms140713763.

Mohamed AR et al. 2018. Deciphering the nature of the coral-*Chromera* association. ISME J. 12:776–790. doi: 10.1038/s41396-017-0005-9.

Moore RB et al. 2008. A photosynthetic alveolate closely related to apicomplexan parasites. Nature. 451:959–963. doi: 10.1038/nature06635.

Müller S, Kappes B. 2007. Vitamin and cofactor biosynthesis pathways in *Plasmodium* and other apicomplexan parasites. Trends Parasitol. 23:112–121. doi: 10.1016/j.pt.2007.01.009.

Nash EA, Nisbet RER, Barbrook AC, Howe CJ. 2008. Dinoflagellates: a mitochondrial genome all at sea. Trends Genet. 24:328–335. doi: 10.1016/j.tig.2008.04.001.

bioRxiv preprint doi: https://doi.org/10.1101/603555; this version posted April 9, 2019. The copyright holder for this preprint (which was not certified by peer review) is the author/funder, who has granted bioRxiv a license to display the preprint in perpetuity. It is made available under aCC-BY-NC-ND 4.0 International license.

Németh E, Nagy Z, Pécsváradi A. 2018. Chloroplast glutamine synthetase, the key regulator of nitrogen metabolism in wheat, performs its role by fine regulation of enzyme activity via negative cooperativity of Its subunits. Front. Plant Sci. 9:191. doi: 10.3389/fpls.2018.00466.

Neuhaus HE, Emes MJ. 2000. Nonphotosynthetic metabolism in plastids. Annu. Rev. Plant Physiol. Plant Mol. Biol. 51:111–140. doi: 10.1146/annurev.arplant.51.1.111.

Nguyen LT, Schmidt HA, Von Haeseler A, Minh BQ. 2015. IQ-TREE: A fast and effective stochastic algorithm for estimating maximum-likelihood phylogenies. Mol. Biol. Evol. 32:268–274. doi: 10.1093/molbev/msu300.

Oborník M. 2019. In the beginning was the word: How terminology drives our understanding of endosymbiotic organelles. Microb. Cell. 6:134–141. doi: 10.15698/mic2019.02.669.

Oborník M et al. 2012. Morphology, ultrastructure and life cycle of *Vitrella brassicaformis* n. sp., n. gen., a novel chromerid from the Great Barrier Reef. Protist. 163:306–323. doi: 10.1016/j.protis.2011.09.001.

Oborník M. 2018. The birth of red complex plastids: One, three, or four times? Trends Parasitol. 34:923–925. doi: 10.1016/j.pt.2018.09.001.

Oborník M, Janouškovec J, Chrudimský T, Lukeš J. 2009. Evolution of the apicoplast and its hosts: From heterotrophy to autotrophy and back again. Int. J. Parasitol. 39:1–12. doi: 10.1016/j.ijpara.2008.07.010.

Oborník M, Lukeš J. 2013. Cell biology of chromerids: Autotrophic relatives to apicomplexan parasites. Int. Rev. Cell Mol. Biol. 306:333–369. doi: 10.1016/B978-0-12-407694-5.00008-0.

Oborník M, Lukeš J. 2015. The organellar genomes of *Chromera* and *Vitrella*, the phototrophic relatives of apicomplexan parasites. Annu. Rev. Microbiol. 69:129–144.

bioRxiv preprint doi: https://doi.org/10.1101/603555; this version posted April 9, 2019. The copyright holder for this preprint (which was not certified by peer review) is the author/funder, who has granted bioRxiv a license to display the preprint in perpetuity. It is made available under aCC-BY-NC-ND 4.0 International license.

doi: 10.1146/annurev-micro-091014-104449.

Oppenheim RD et al. 2014. BCKDH: The missing link in apicomplexan mitochondrial metabolism is required for full virulence of *Toxoplasma gondii* and *Plasmodium berghei*. PLoS Pathog. 10:e1004263. doi: 10.1371/journal.ppat.1004263.

Pagliarini DJ, Rutter J. 2013. Hallmarks of a new era in mitochondrial biochemistry. Genes Dev. 27:2615–2627. doi: 10.1101/gad.229724.113.

Palmfeldt J, Bross P. 2017. Proteomics of human mitochondria. Mitochondrion. 33:2–14. doi: 10.1016/j.mito.2016.07.006.

Panigrahi AK et al. 2009. A comprehensive analysis of *Trypanosoma brucei* mitochondrial proteome. Proteomics. 9:434–450. doi: 10.1002/pmic.200800477.

Patron NJ, Waller RF. 2007. Transit peptide diversity and divergence: A global analysis of plastid targeting signal. BioEssays. 29:1048–1058. doi: 10.1002/bies.20638.

Petersen J et al. 2014. *Chromera velia*, endosymbioses and the rhodoplex hypothesis - Plastid evolution in cryptophytes, alveolates, stramenopiles, and haptophytes (CASH lineages). Genome Biol. Evol. 6:666–684. doi: 10.1093/gbe/evu043.

Petersen TN, Brunak S, von Heijne G, Nielsen H. 2011. SignalP 4.0: discriminating signal peptides from transmembrane regions. Nat. Methods. 8:785–786. doi: 10.1038/nmeth.1701.

Petsalaki EI, Bagos PG, Litou ZI, Hamodrakas SJ. 2006. PredSL: A tool for the N-terminal sequence-based prediction of protein subcellular localization. Genomics, Proteomics Bioinforma. 4:48–55. doi: 10.1016/S1672-0229(06)60016-8.

Sazanov LA, Jackson JB. 1994. Proton-translocating transhydrogenase and NAD- and NADP-linked isocitrate dehydrogenases operate in a substrate cycle which contributes to fine regulation of the tricarboxylic acid cycle activity in mitochondria. FEBS Lett. 344:109–116. doi: 10.1016/0014-5793(94)00370-X.

bioRxiv preprint doi: https://doi.org/10.1101/603555; this version posted April 9, 2019. The copyright holder for this preprint (which was not certified by peer review) is the author/funder, who has granted bioRxiv a license to display the preprint in perpetuity. It is made available under aCC-BY-NC-ND 4.0 International license.

Schleiff E, Soll J, Küchler M, Kühlbrandt W, Harrer R. 2003. Characterization of the translocon of the outer envelope of chloroplasts. J. Cell Biol. 160:541–551. doi: 10.1083/jcb.200210060.

Searcy DG. 2003. Metabolic integration during the evolutionary origin of mitochondria. Cell Res. 13:229–238. doi: 10.1038/sj.cr.7290168.

Shanmugasundram A, Gonzalez-Galarza FF, Wastling JM, Vasieva O, Jones AR. 2013. Library of Apicomplexan Metabolic Pathways: A manually curated database for metabolic pathways of apicomplexan parasites. Nucleic Acids Res. 41:706–713. doi: 10.1093/nar/gks1139.

Smith DGS et al. 2007. Exploring the mitochondrial proteome of the ciliate protozoon *Tetrahymena thermophila*: Direct analysis by tandem mass spectrometry. J. Mol. Biol. 374:837–863. doi: 10.1016/j.jmb.2007.09.051.

Sobotka R et al. 2017. Extensive gain and loss of photosystem I subunits in chromerid algae, photosynthetic relatives of apicomplexans. Sci. Rep. 7:13214. doi: 10.1038/s41598-017-13575-x.

Stitt M. 2002. Steps towards an integrated view of nitrogen metabolism. J. Exp. Bot. 53:959–970. doi: 10.1093/jexbot/53.370.959.

Sun S, Habermann BH. 2017. A guide to computational methods for predicting mitochondrial localization. In: Mitochondria: Practical protocols. Mokranjac, D & Perocchi, F, editors. Springer New York: New York, NY pp. 1–14. doi: 10.1007/978-1-4939-6824-4_1.

Terashima M, Specht M, Hippler M. 2011. The chloroplast proteome: A survey from the *Chlamydomonas reinhardtii* perspective with a focus on distinctive features. Curr. Genet. 57:151–168. doi: 10.1007/s00294-011-0339-1.

Tetlow IJ, Rawsthorne S, Raines C, Emes MJ. 2005. Plastid metabolic pathways. In:

bioRxiv preprint doi: https://doi.org/10.1101/603555; this version posted April 9, 2019. The copyright holder for this preprint (which was not certified by peer review) is the author/funder, who has granted bioRxiv a license to display the preprint in perpetuity. It is made available under aCC-BY-NC-ND 4.0 International license.

Annual Plant Reviews. Møller, SG, editor. Vol. 13 Blackwell Publishing Ltd pp. 60–125. doi: 10.1002/9781119312994.apr0123.

Tikhonenkov D V. et al. 2014. Description of *Colponema vietnamica* sp.n. and *Acavomonas peruviana* n. gen. n. sp., two new alveolate phyla (Colponemidia nom. nov. and Acavomonidia nom. nov.) and their contributions to reconstructing the ancestral state of alveolates and eukaryotes Gribaldo, S, editor. PLoS One. 9:e95467. doi: 10.1371/journal.pone.0095467.

Tomčala A, Michálek J, Schneedorferová I, Füssy Z, Oborník M. *De novo* fatty acid biosynthesis in phototrophic apicomplexan relatives *Chromera velia* and *Vitrella brassicaformis*. unpublished.

Tymoshenko S et al. 2015. Metabolic needs and capabilities of *Toxoplasma gondii* through combined computational and experimental analysis. PLoS Comput. Biol. 11:e1004261. doi: 10.1371/journal.pcbi.1004261.

Vazač J, Füssy Z, Hladová I, Killi S, Oborník M. 2017. Ploidy and number of chromosomes in the alveolate alga *Chromera velia*. Protist. 169:53–63. doi: 10.1016/j.protis.2017.12.001.

Wiedemann N, Pfanner N. 2017. Mitochondrial machineries for protein import and assembly. Annu. Rev. Biochem. 86:685–714. doi: 10.1146/annurev-biochem-060815-014352.

van Wijk KJ, Baginsky S. 2011. Plastid proteomics in higher plants: Current state and future goals. Plant Physiol. 155:1578–1588. doi: 10.1104/pp.111.172932.

Woehle C, Dagan T, Martin WF, Gould SB. 2011. Red and problematic green phylogenetic signals among thousands of nuclear genes from the photosynthetic and apicomplexa-related *Chromera velia*. Genome Biol. Evol. 3:1220–1230. doi: 10.1093/gbe/evr100.

Woo YH et al. 2015. Chromerid genomes reveal the evolutionary path from

bioRxiv preprint doi: https://doi.org/10.1101/603555; this version posted April 9, 2019. The copyright holder for this preprint (which was not certified by peer review) is the author/funder, who has granted bioRxiv a license to display the preprint in perpetuity. It is made available under aCC-BY-NC-ND 4.0 International license.

photosynthetic algae to obligate intracellular parasites. eLife. 4:e06974. doi: 10.7554/eLife.06974.

Yoo H, Antoniewicz MR, Stephanopoulos G, Kelleher JK. 2008. Quantifying reductive carboxylation flux of glutamine to lipid in a brown adipocyte cell line. J. Biol. Chem. 283:20621–20627. doi: 10.1074/jbc.M706494200.

Zhu G et al. 2004. Expression and functional characterization of a giant Type I fatty acid synthase (CpFAS1) gene from *Cryptosporidium parvum*. Mol. Biochem. Parasitol. 134:127–135. doi: 10.1016/j.molbiopara.2003.11.011.

FIGURES:

Figure 1: Overview of reference pathways, focused on the inter-connected reactions of terpenoid, lipid and tetrapyrrole biosynthesis, mitochondrial sulfur assimilation and glycine cleavage, and ribosomal proteins. Pathways are color-coded and enzymes/proteins are numbered according to the Supplementary Table S1. Abbreviations: ACP – acyl-carrier protein, ALA – delta-aminolevulinic acid, Chl *a* – chlorophyll *a*, DGDG – digalactosyldiacylglycerolipids, DHAP – dihydroxyacetone phosphate, GGPP – geranylgeranyl pyrophosphate, IMS – inter-membrane space, MEP – methyl-D-erythritol 4-phosphate, PEP – phospho*enol*pyruvate, pyr – pyruvate, SQDG – sulfoquinovosyldiacylglycerolipids, THF – tetrahydrofolate.

Figure 2: Overview of reference pathways, continued, focused on the inter-connected reactions of carbohydrate and amino acid biosynthesis, mitochondrial respiration and plastid photosynthesis. Pathways are color-coded and enzymes/proteins are numbered or coded according to the Supplementary Table S1. 2-

bioRxiv preprint doi: https://doi.org/10.1101/603555; this version posted April 9, 2019. The copyright holder for this preprint (which was not certified by peer review) is the author/funder, who has granted bioRxiv a license to display the preprint in perpetuity. It is made available under aCC-BY-NC-ND 4.0 International license.

OG – 2-oxoglutarate, DHAP – dihydroxyacetone phosphate, Ery-4P – erythrose 4-phosphate, FAD – flavin adenine dinucleotide, IMS – inter-membrane space, OAA – oxaloacetate, orn – ornithine, PEP – phospho*enol*pyruvate, PQ – plastoquinol, PRPP – 5-phosphoribosyl-1-pyrophosphate, pyr – pyruvate, Ru-5P – ribulose 5-phosphate, TCA – tricarboxylic acid, THF – tetrahydrofolate, UQ – ubiquinone.

Figure 3: Sequence motifs surrounding the signal cleavage site differ in chromerids. While *C. velia* retains a highly conserved Phe residue that follows after the cleavage site (marked by +1), in *V. brassicaformis* an Ala residue is more conserved. Since orthologous sequences were mostly used for reference dataset compilation, it is likely that this change reflects changes in transit peptide recognition of proteins e*n route* to the plastid stroma. Logoplot created by WebLogo (Crooks et al. 2004).

Table 1: Performance of various localization predictors as employed in this study. ASAFind and HECTAR-plastid were used for plastid reference assessment. Note that ASAFind has a cumulative score, with our data reaching up to values of 6. ASAFind+ denotes ASAFind with species-specific bit score matrices designed with *C. velia* and *V. brassicaformis* plastid references. TargetP, HECTAR-mitochondrion and MultiLoc2 were used for mitochondrial predictions and two thresholds are presented for these predictors, one aimed at higher sensitivity (s – 75%), the other aimed at high precision (p – 85%).

SUPPLEMENTARY MATERIAL:

Supplementary Table S1: Reference protein lists grouped by metabolic function.

bioRxiv preprint doi: https://doi.org/10.1101/603555; this version posted April 9, 2019. The copyright holder for this preprint (which was not certified by peer review) is the author/funder, who has granted bioRxiv a license to display the preprint in perpetuity. It is made available under aCC-BY-NC-ND 4.0 International license.

Supplementary Table S2: Prediction scores for reference proteins and the species-specific ASAFind scoring matrices of *C. velia* and *V. brassicaformis*.

Supplementary Figure S3: Targeting peptide score distributions for reference sequences. Reference colors: green – plastid, blue – mitochondrial, grey – other (cytosolic or non-plastid endomembrane route).

Supplementary Data S4: Inferred phylogenies of argJ, polyprenyl-PP synthases, and PRPP synthase; set of updated reference protein sequences. Trees in Newick format, accessions are marked on leaves. The maximum-likelihood trees were inferred by the IQ-TREE software (see Methods). Sequence updates are based on homology searches within alternative transcriptomic datasets (elongated sequences) and comparison of orthologous sequences in *C. velia* and *V. brassicaformis* (merged contigs). [now part of Supplementary Table S1]

bioRxiv preprint doi: https://doi.org/10.1101/603555; this version posted April 9, 2019. The copyright holder for this preprint (which was not certified by peer review) is the author/funder, who has granted bioRxiv a license to display the preprint in perpetuity. It is made available under aCC-BY-NC-ND 4.0 International license.

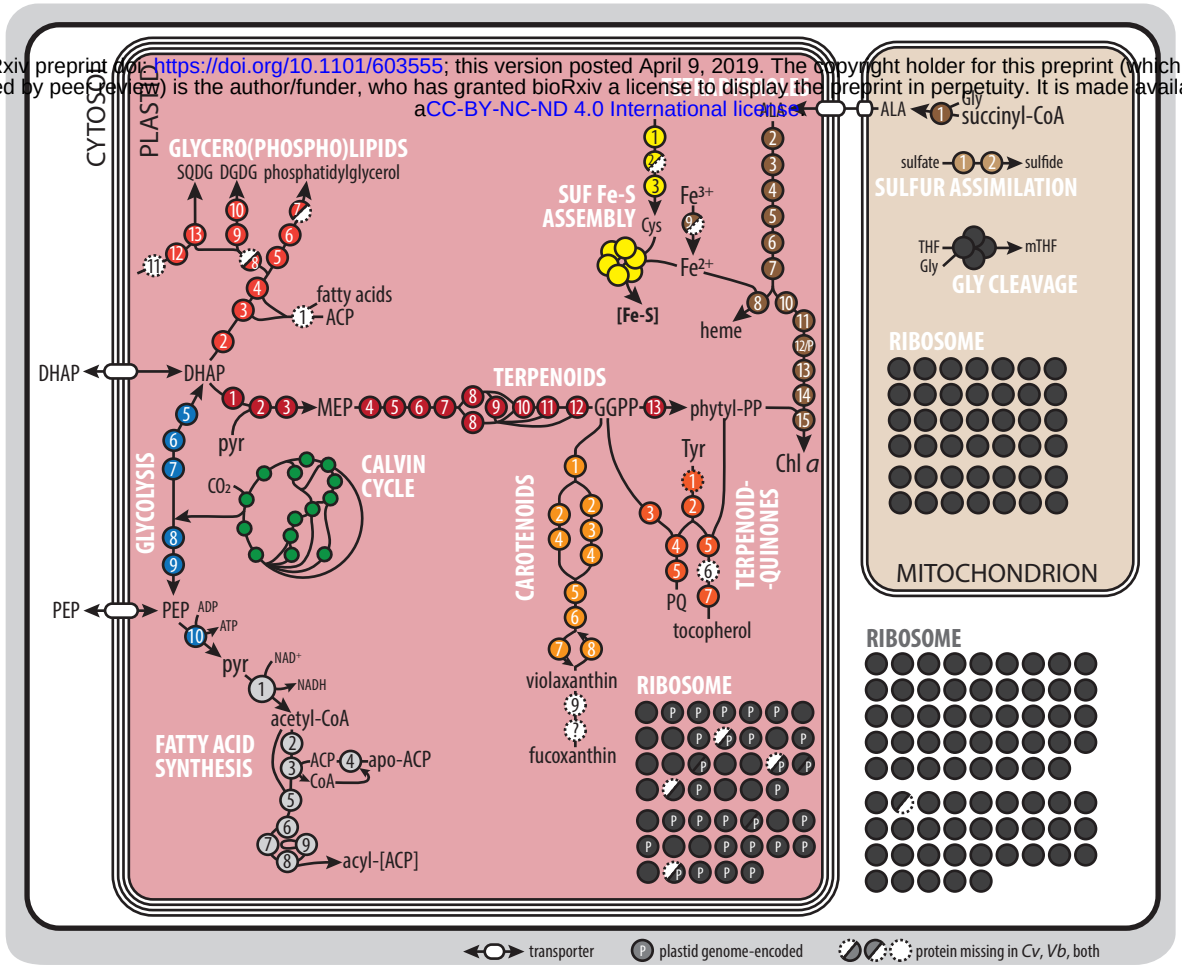

bioRxiv preprint doi: https://doi.org/10.1101/603585 This version posted April 9, 2019. The copyright holder for this preprint (which was not certified by peer review) is the author/funder, who has granted bioRxiv a license to display the preprint in perpetuity. It is made available under CC-BY-NC-ND 4.0 International license.

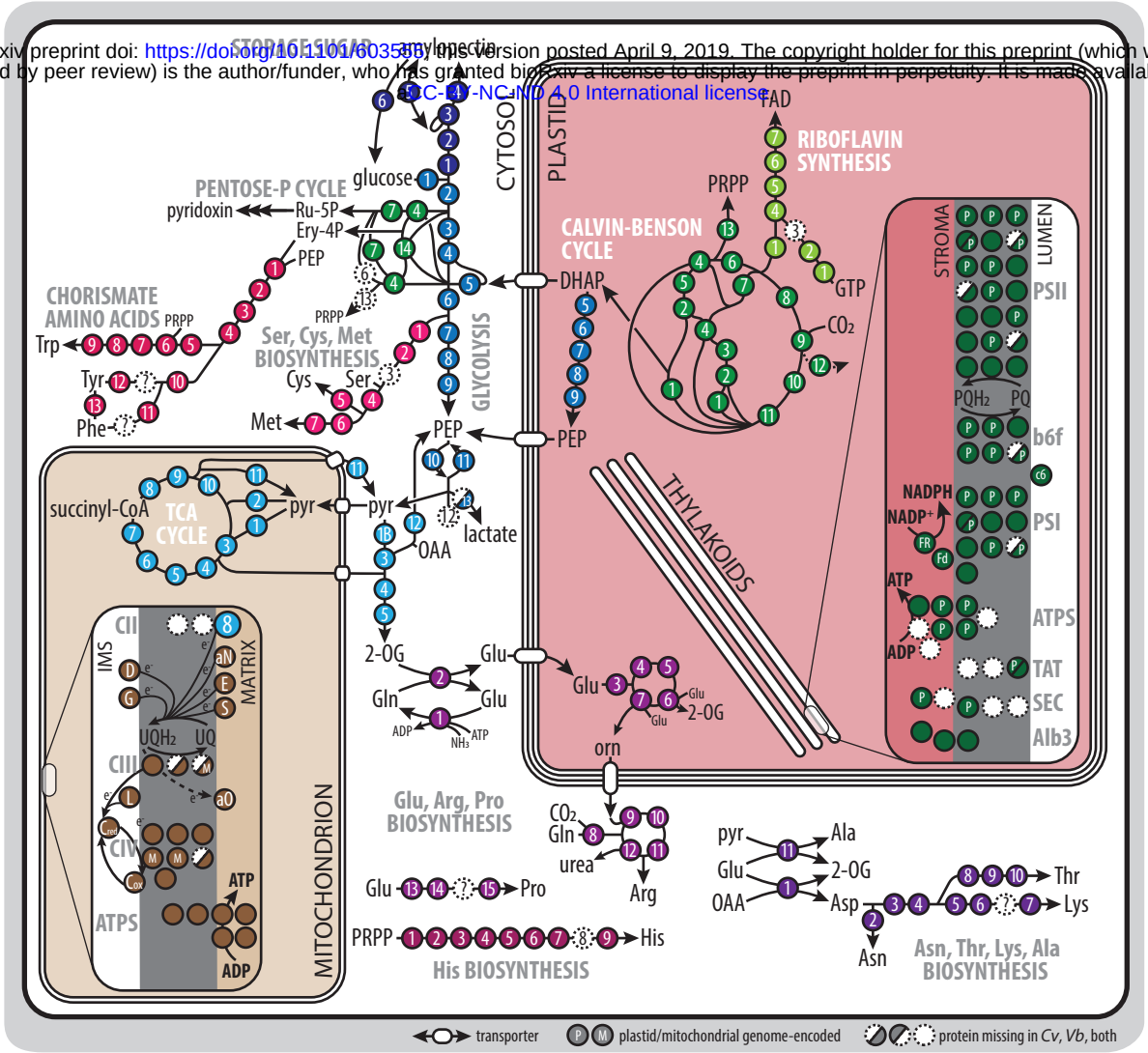

bioRxiv preprint doi: https://doi.org/10.1101/603555; this version posted April 9, 2019. The copyright holder for this preprint (which was not certified by peer review) is the author/funder, who has granted bioRxiv a license to display the preprint in perpetuity. It is made available under aCC-BY-NC-ND 4.0 International license.

Chromera velia

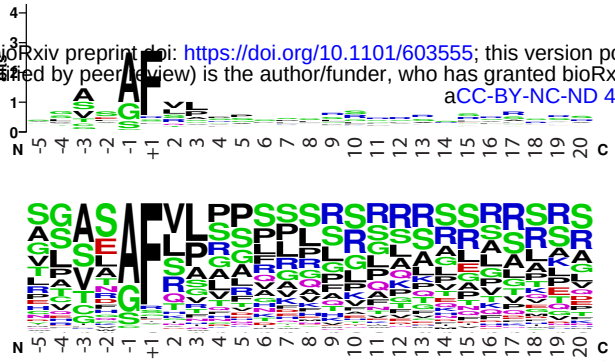

Vitrella brassicaformis

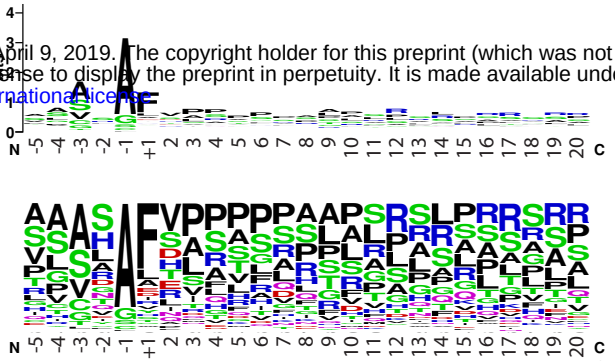

	ASAFind	ASAFind+	HECTAR	TargetP - mTP		HECTAR - mTP		MultiLoc2 - mTP	
C. velia				(s)	(p)	(s)	(p)	(s)	(p)
THRESHOLD:	1.4	1.4	0.05	0.35	0.8	0.14	0.41	0.25	0.95
SENSITIVITY:	0.770	0.826	0.765	0.757	0.586	0.748	0.586	0.748	0.361
PRECISION:	0.921	0.921	0.872	0.375	0.844	0.529	0.855	0.485	0.736
V. brassicaformis									
THRESHOLD:	1	1	0.16	0.56	0.81	0.18	0.37	0.64	0.89
SENSITIVITY:	0.758	0.897	0.747	0.757	0.586	0.748	0.559	0.755	0.582
PRECISION:	0.886	0.916	0.967	0.712	0.855	0.664	0.861	0.697	0.842